

**Fractionating executive control in the human brain:
A within-subjects fMRI study**

Sabrina Lemire-Rodger

A THESIS SUBMITTED TO
THE FACULTY OF GRADUATE STUDIES
IN PARTIAL FULFILLMENT OF THE REQUIREMENTS
FOR THE DEGREE OF
MASTER'S OF ARTS

GRADUATE PROGRAM IN CLINIAL PSYCHOLOGY
YORK UNIVERSITY
TORONTO, ONTARIO

September 2014

© Sabrina Lemire-Rodger, 2014

Abstract

Executive control processes have been found to cluster around three factors: updating, inhibition and task switching. However, few studies have directly investigated the fractionation of executive control in the brain, and none have examined convergent and divergent patterns of neural activity for all three using matched tasks in a single scanning protocol. Using a novel paradigm that manipulates executive control demands while keeping other task demands constant, we directly assessed the dissociability of the neural correlates of updating, inhibition and task switching. Our analyses revealed diverse patterns of brain activity associated with each executive control process. Though several interpretations of the data are considered, our results provide strong evidence that executive functions are dissociable at the level of the brain.

Dedication

This thesis is dedicated to the brilliant women of my cohort: Areeba, Chrissy, Farena, Holly, Katie, Khuraman, Leah, Molly and Samantha, who have set the bar formidably high, and have genially encouraged each other to reach beyond it.

Acknowledgements

The author wishes to thank the individuals who made this project possible: Dr. Gary Turner for his supportive supervision throughout this experiment; Dr. Shayna Rosenbaum for her conceptual input and support; Dr. Dale Stevens for his feedback and suggestions regarding analyses; Dr. Nathan Spreng for his role in originating the project and his feedback; Joy Williams for operating the scanner and for being exceedingly helpful and accommodating throughout testing; Benjamin Cassidy for his help with participant recruitment and valuable support; Joseph Viviano for his dedicated work building the pre-processing pipeline, for his help with all aspects of neuroimaging data handling and for his insightful input; Karin Kantarovich for contributing to participant testing; Dhawal Selarka for developing early versions of the paradigm; Jasmin Amin for help with E-Prime; Areeba Adnan for contributing support, encouragement and insight at all stages of the project; and my husband Rizwan Jiwan for his help with coding and data analysis, as well as for his patience and ongoing support.

Author's Contribution

The author, Sabrina Lemire-Rodger, was involved in all aspects of the experiment.

Sabrina Lemire-Rodger contributed to the creation of the study conceptually, specifically designing the task paradigm and creating it using E-Prime. The author carried out a neuroimaging pilot study for the paradigm, where she recruited and ran all participants (Dhawal Selarka completed a behavioural pilot study of the paradigm). With the help of

Benjamin Cassidy, Sabrina Lemire-Rodger recruited all participants for the current study.

The author, along with Karin Kantarovich, tested the participants. Sabrina Lemire-Rodger and Joseph Viviano completed the pre-processing of the neuroimaging data. Sabrina Lemire-Rodger analyzed the behavioural data using SPSS and the neuroimaging data using PLS. All tables and figures were created by Sabrina Lemire-Rodger. Interpretation of the findings was carried out by the author, with the help of Dr. Gary Turner.

TABLE OF CONTENTS

Abstract.....	ii
Dedication.....	iii
Acknowledgments.....	iv
Author’s Contribution.....	v
Table of Contents.....	vi
List of Tables.....	vii
List of Figures.....	viii
List of Supplementary Materials.....	ix
List of Abbreviations.....	x
Introduction	1
Methods.....	8
Participants.....	8
Experimental Procedure.....	8
Control task.....	9
Updating task.....	9
Inhibition task.....	9
Combined updating & inhibition task.....	10
Task switching.....	10
Overall structure of the experiment.....	11
MRI Data Acquisition and Pre-Processing.....	12
Data Analysis.....	13
Results.....	14
Behavioral Results.....	14
Accuracy.....	15
Reaction time.....	16
Neuroimaging Results.....	17
Full-model analysis.....	18
Individual updating analysis.....	18
Individual inhibition analysis.....	19
Individual task switch analysis.....	19
Conjunction of individual analyses.....	19
Discussion.....	20
Full-Model.....	20
Individual Executive Processes.....	25
Updating.....	25
Inhibition.....	26
Task switching.....	27
Conjunction analysis.....	28
Study Limitations.....	29
Future Directions.....	30
Conclusion.....	31
References.....	34
Appendices.....	43

List of Tables

Table 1: Number of Trials per Condition.....	43
Table 2: Mean Accuracy and Reaction Times.....	44
Table 3: Paired <i>t</i> -tests for % Accuracy.....	45
Table 4: Paired <i>t</i> -tests for mean RT.....	46
Table 5: Cluster reports for LV1 & LV2 of the Full-Model PLS Analysis.....	47
Table 6: Cluster reports for Control & Updating Analysis.....	48
Table 7: Cluster reports for the Control & Inhibition Analysis.....	49
Table 8: Cluster reports for he Control & Task Switching Analysis.....	50

List of Figures

Figure 1: Overview of the different tasks used in the study.....	51
Figure 2: Overview of the structure of a run.....	52
Figure 3: LV1 from the full-model analysis.....	53
Figure 4: LV2 from the full-model analysis.....	54
Figure 5: LV1 from the control & updating analysis.....	55
Figure 6: LV1 from the control & inhibition analysis.....	56
Figure 7: LV1 for the control & task switch analysis.....	57
Figure 8: Conjunction analysis results.....	58

List of Supplementary Materials

Supplementary Table 1: Paired Wilcoxon Signed Rank test for % Accuracy.....	59
Supplementary Table 2: Paired <i>t</i> -tests for median RT.....	60
Supplementary Table 3: Full Cluster report for LV1 from the Full-Model PLS Analysis.....	61
Supplementary Table 4: Full Cluster report for LV2 from the Full-Model PLS Analysis.....	62
Supplementary Table 5: Full Cluster report for LV1 from the Updating & Control PLS Analysis.....	64
Supplementary Table 6: Full Cluster report for LV1 from the Inhibition & Control PLS Analysis.....	66
Supplementary Table 7: Full Cluster report for LV1 from the Task Switch & Control PLS Analysis.....	68
Supplementary Figure 1: Brain patterns for LV1 from the full-model PLS analysis for all lags.....	69
Supplementary Figure 2: Brain patterns for LV2 from the full-model PLS analysis for all lags.....	70
Supplementary Figure 3: Brain patterns for LV1 from the updating & control PLS analysis for all lags.....	71
Supplementary Figure 4: Brain patterns for LV1 from the Inhibition & control PLS analysis for all lags.....	72
Supplementary Figure 5: Brain patterns for LV1 from the task switch & control PLS analysis for all lags.....	73

List of Abbreviations

ACC – Anterior Cingulate Cortex
AFNI – Analysis of Functional NeuroImages
ANOVA – Analysis of Variance
BOLD – Blood Oxygen Level Dependent
BSR – Bootstrap Ratio
DLPFC – Dorsolateral Prefrontal Cortex
EPI – Echo Planar Images
fMRI – functional Magnetic Resonance Imaging
IFJ – Inferior Frontal Junction
IFG – Inferior Frontal Gyrus
IPL – Inferior Parietal Lobule
LV – Latent Variable
MRI – Magnetic Resonance Imaging
MP-RAGE - Multi-Planar Rapid Gradient Echo
MNI – Montreal Neurological Institute
MFG – Middle Frontal Gyrus
PLS – Partial Least Squares
RT – Reaction Time
PFC – Prefrontal Cortex
pre-SMA – pre-Supplementary Motor Area
SMA – Supplementary Motor Area
SPSS – Statistical Package for the Social Sciences
URPP – Undergraduate Research Participant Pool
VLPFC – Ventrolateral Prefrontal Cortex
WCST – Wisconsin Card Sorting Task

Fractionating executive control in the human brain: A within-subjects fMRI study

The capacity to set, pursue, and attain future goals is a fundamental to the human experience. Bridging the temporal divide between intention and action requires maintaining goals in mind, flexibly adapting behaviours to match shifting environmental contingencies and inhibiting distractions. These cognitive capacities are typically subsumed under the umbrella of 'executive functions' and have been associated with the functioning of the frontal lobes and their associated networks. There has been considerable debate as to whether executive functioning reflects a unitary cognitive construct, or in fact represents dissociable cognitive processes, grouped together based on their historical association with the frontal lobes and frontally mediated systems (Alvarez & Emory, 2006).

There is evidence for a more unitary view of executive functioning, in which different types of complex, executive tasks are carried out by a common underlying cognitive mechanism, akin to general intelligence (Duncan et al., 2000). At the level of the brain, this view holds that executive control relies on an established neural network, common to all "higher-level" processing and recruited by various cognitive demands (e.g., Braver, Paxton, Locke & Barch, 2009, Duncan & Owen, 2000; Duncan et al., 2000; Niendam et al., 2012). This common network of activation is often referred to as the frontoparietal control network and is made up of nodes within prefrontal and parietal cortices (Duncan & Owen, 2000; Spreng, Sepulcre, Turner, Stevens & Schacter, 2013; Vincent, Kahn, Snyder, Raichle, & Buckner, 2008).

There is also evidence that a variety of component processes interact to make "higher-order" cognition possible, and support the idea that executive function is

fractionable and better conceptualized as a “macroconstruct” (Zelazo, Carter, Reznick, & Frye, 1997; Alvarez & Emory, 2006). The view that executive functions are dissociable is also supported at the level of the brain (McNab, Leroux, Strand, Thorell, Bergman, & Klingberg, 2008; Stuss & Alexander, 2000; Wager, Jonides & Reading, 2004). In a seminal report, Miyake, Friedman, Emerson, Witzki and Howerter (2000), set out to address this unitary versus fractionation question empirically using a series of standardized and experimental executive function measures postulated to measure performance in 3 executive control domains: (i) working memory - the ability to hold, manipulate and update information in the mind, (ii) shifting – mental flexibility, the ability to switch tasks or mental set, and (iii) inhibition – the ability to withhold inappropriate responses and suppress irrelevant information. Testing over 200 healthy, young adults the authors used a confirmatory factor analysis to examine whether the pattern of performance across all tasks was better represented by a unitary, single-factor model or by a dissociable, three-factor model. Their data provided strong support for the 3-factor model suggesting that executive functioning could indeed be fractionated into at least three dissociable processes.

However, there are myriad views on how these three processes relate to each other, as well as their relative contributions to overall executive functioning. For example, some consider mental flexibility and the ability to shift tasks to be a combination of working memory and inhibition, rather than an independent cognitive control process (e.g., Diamond, 2013). In a commonly cited cognitive model of working memory, executive control subserves working memory (Baddeley, 1992). The superordinate category is not executive control, but working memory itself. Inhibition is also considered

by many to be an important component of working memory (e.g., Hanania & Smith, 2010; Hasher, & Zacks, 1988; Zanto & Gazzaley, 2009), rather than an independent process. Similarly, it is possible that task switching, or shifting of cognitive set, is simply another form of inhibition, the ability to suppress the previous set and resist the impulse to act on currently irrelevant information.

Despite the diverse theories on how these three executive processes dovetail, the three-factor model of dissociable executive control processes proposed by Miyake and colleagues (2000) has remained influential in guiding both behavioural and neuroimaging investigations of executive functioning. Several studies have examined the neural basis of each executive process. It is widely accepted that updating relies on the lateral prefrontal cortex (PFC) (D'Esposito, Postle, & Rypma, 2000). Meta-analyses of working memory studies have found that tasks requiring continuous updating (such as the n-back task) selectively engage the dorsolateral prefrontal cortex (DLPFC), the premotor cortex, and the frontal poles (Owen, McMillan, Laird, Bullmore, 2005; Wager & Smith, 2003). Inhibition has been found to rely mainly on the inferior frontal gyrus, particularly in the right hemisphere, and pre-supplementary motor area (pre-SMA) (Chambers, Garavan & Bellgrove, 2009; Simmonds, Pekar & Mostofsky, 2008). Meta-analyses of task switching studies have found a wide-ranging network of reliable areas of activation including the DLPFC, superior medial PFC, insula, posterior parietal cortex, as well as activity in the visual cortex (Buchsbaum, Greer, Chang, & Berman, 2005; Kim Cilles, Johnson, & Gold, 2012; Wager, Jonides & Reading 2004). Notwithstanding the large body of literature on each executive process independently, few neuroimaging studies have examined

executive functioning by considering more than a single executive control processes at a time.

In the case of updating and inhibition, McNab, Leroux, Strand, Thorell, Bergman and Klingberg (2008) used various established working memory and inhibition tasks to assess the common regions of activation between these two processes. They found that both executive control processes recruited the right inferior frontal gyrus, right middle frontal gyrus and the right parietal lobe. Though they focused on commonalities rather than dissociation, the patterns of overall brain activity related to each process were distinct (updating was associated with a larger and more dorsal pattern of activation than inhibition). In their meta-analysis of updating and inhibition studies across the lifespan, Turner and Spreng (2012) found reliable recruitment of lateral PFC, posterior parietal and subcortical regions in younger adults for studies of working memory. In the case of inhibition, their analysis revealed inferior frontal gyrus, supplementary motor area, posterior parietal, DLPFC, and insular activity. Again, this represented separate, but overlapping networks.

Other studies have directly compared the neural basis of inhibition and task switching. Using a go/wait paradigm, Swainson and colleagues (2003) were able to assess both inhibition and task switching mechanisms in a single task. They found anterior cingulate activation for both task switching and inhibition. They argue that lateral PFC activation is related to task switching rather than inhibitory demands, which are limited to the right inferior frontal sulcus (Swainson et al., 2003). Also using a within-subject single task design, Sylvester et al. (2003) determined that switching recruits left parietal and bilateral extrastriate cortex, whereas inhibition recruits right premotor cortex,

right parietal cortex, and the right frontal pole. Common areas across both switching and inhibition included left DLPFC, medial PFC and bilateral parietal lobes. Finally, as part of their larger meta-analysis of neuroimaging studies of the Wisconsin Card Sorting Task (WCST), Buchsbaum et al. (2005) carried out meta-analyses of the switching and inhibition literature. Though both processes were compared to the WCST and not to each other, there were apparent differences between these two sub-processes. Switching was associated with a typical frontoparietal pattern of activation, as well as additional areas of activation in the occipital and temporal lobes. There were fewer areas of activation associated with inhibition, the most robust of which was the inferior frontal gyrus in the right hemisphere. Buchsbaum et al. (2005) also found that both task switching and inhibition share profiles of activation with the WCST.

While there are no empirical studies comparing the basis of task switching and updating, there has been one meta-analytic review that has examined the neural basis of task switching and its overlap with working memory (Wager et al., 2004). The common network of executive function activity identified in that study included medial PFC, precuneus, inferior parietal lobules, and premotor cortex. Activity in the left extrastriate cortex and the right parietal lobe was unique to task switching. Executive working memory tasks, such as continuous updating, selectively recruited the anterior and dorsolateral PFC. Overall, these studies find common areas of activation between different executive processes in the medial and lateral PFC as well as the posterior parietal lobes, though these areas of overlap shift slightly based on which processes are being compared.

There are no studies, to our knowledge, that have considered all three executive control processes within a single experiment, or that have empirically tested the fractionation hypothesis by manipulating executive control demands within a standard task architecture. The tasks commonly used to assess executive functioning represent a limitation of the current body of literature on the neural basis of executive control processes. Many tasks that are meant to challenge the same executive function often have low behavioural correlations between them, due to the idiosyncrasies of different tasks (Friedman and Miyake 2004, McNab et al., 2008). Moreover, standard measures of executive functioning have been found to have relatively low reliability and inadequate validity (Alvarez & Emory, 2006).

Miyake and colleagues (2000) acknowledged that there is a task impurity problem when studying the fractionation of executive functions. The individual tasks used in their study were drawn from a vast experimental and clinical neuropsychological literature. In addition to their a priori selection based on (purportedly) different executive control demands the tasks also varied across multiple dimensions including visuospatial and motor response demands, access to verbal mediation, speeded processing, etc. While these variable demands were incorporated as part of the factor-analytic approach, and indeed served to strengthen findings of common 'executive' factors amongst seemingly disparate tasks, the possibility remains that other common task demands may have contributed to the observed factor structure. Similarly, while the findings of the neuroimaging studies reviewed above are consistent with a dissociable model of executive functioning, at least at the level of the brain, lack of a common task architecture allowing for direct within-subject contrasts of specific executive control

processes, leaves open the possibility that any difference found between the neural correlates of each executive process is due to the idiosyncrasies of each task, rather than differences in executive control demands. In the present study, we set out to empirically test the three-factor model of executive control at the level of the brain using a standard task architecture and a within-subject experimental design. Specifically, we investigated whether the executive control functions postulated by Miyake et al. (2000) were associated with discrete patterns of functional brain activation, particularly within frontal brain regions and frontally mediated brain networks. To achieve this, we developed a novel paradigm specifically designed to investigate the dissociability of executive control functions at the level of the brain using functional magnetic resonance imaging (MRI) methods. This novel experimental paradigm carefully controlled perceptual, motor and 'non-executive' cognitive demands (e.g., language, semantic representations) across all conditions. By matching bottom-up (i.e., non-executive) demands and manipulating top-down (i.e., executive control) processes in a single experimental paradigm, we were able to precisely assess and directly compare each executive function.

We hypothesized that each executive control task would be associated with differentiated patterns of neural activation and that these patterns of activation would overlap, as reported in previous studies that contrasted two executive processes at a time. To test this hypothesis, we chose to use a data-driven, multivariate approach (Partial Least Squares – PLS, Krishnan et al., 2011), rather than a univariate approach, in analyzing the neuroimaging data. This enabled us to examine the patterns of brain activity that emerged based on our experimental design without defining a priori

contrasts. We also expected that regions of overlap between the three executive control processes would map onto regions of the frontal and parietal cortices commonly implicated in executive control processes (Dosenbach et al., 2007; Duncan & Owen, 2000; Vincent, Kahn, Snyder, Raichle, & Buckner, 2008), while regions selectively engaged by each individual process would represent areas of specialization, consistent with previous literature.

Methods

Participants

25 healthy young adults (12 women, 13 men, $M_{age} = 22.08$, age range: 18–28 years) were recruited through York University's Undergraduate Research Participant Pool (URPP), the lab database, or word of mouth. Participants recruited through the URPP were awarded course credit for their participation; all other participants were compensated \$50 for their time. Participants had no reported history of psychiatric or neurological illnesses and no ferromagnetic metal in their body. All participants signed an informed consent form and completed an MRI screening procedure before participating in the study. All procedures were approved by the Institutional Review Board of York University and the study was carried out in accordance with the Canadian Tri-Council's code of ethical conduct for research involving humans.

Experimental Procedure

We created a novel paradigm to test updating, inhibition and task switching in a balanced, controlled and consistent way (for behavioural pilot study of this paradigm, see Lemire-Rodger, Selarka & Turner, 2013). Participants were presented with three yellow

or blue squares on a black background. On each trial, participants were required to make a “yes” or “no” response (equivalent to “1” or “2” on a keypad). Perceptual, motor and extraneous cognitive demands were kept constant throughout the experiment. The experiment was created using E-Prime 2.0 (runtime version 2.0.10.242, Psychology Software Tools, Inc.) and presented on a testing-dedicated Dell laptop computer running Windows 8. The experimental design included four conditions, described below:

Control task. In the baseline control condition, participants were asked to attend to the perceptual features of the centre square in the array. Participants were asked to respond to the question, “Is the middle square blue?” They had to press “yes” (button 1) if the middle square was blue, and “no” (button 2) if the middle square was yellow.

Updating task. The updating condition was a continuous two-back task. During this condition, the stimulus array was identical to the control task. However, the participants were now being asked, “Was the middle square blue two trials ago?” Therefore, during this task, participants had to keep information from previous trials in mind to answer correctly. Participants were instructed to press “yes” (button 1) if the middle square two trials prior was blue, and “no” (button 2) if the middle square two trials prior was yellow. Participants were expected to respond on every trial. On the first two trials of this condition, participants were instructed to answer “no,” since there were no two-back trials to consider.

Inhibition task. During the inhibition condition, the participants were again carrying out the baseline control task, answering “Is the middle square blue?” However, they were now asked to withhold their response if two (and only two) of the squares in

the array were yellow. In other words, inhibit trials were those on which any two of the three squares were yellow. On these trials, participants were required to do nothing.

Combined updating & inhibition task. In this condition, the participants were completing the two-back task (“Was the middle square blue two trials ago?”), but they were asked to withhold their response if there were two yellow squares in the current array.

Task switching. Task switching was embedded between the other conditions. During the practice task, the participants were trained to associate a cue screen with each condition (e.g., “2-back” for the updating condition, “double yellow” for the inhibition condition). When the cue screen was presented, participants were required to change the set of rules they were previously using, and engage in the new task indicated by the cue screen. As participants completed a block of trials of one condition (e.g., the control task), a cue screen would be presented for 1000ms (e.g., “2-back”) and then the participants would complete a set of trials using the currently relevant rules. For example, if they had seen “2-back,” participants were then expected to engage in the updating task, answering “no” for the first two trials, since they were told to start each block anew. They did not need to keep the stimuli from the previous block in mind – this ensured we kept each condition as isolated as possible. The first trial of a new block of trials was flagged as the *task switch trial*, where the cognitive costs associated with shifting were predicted to occur (in line with previous literature on task switching and confirmed in our behavioural pilot study). The trial immediately following the cue screen was modeled as a task-switching event (see Figure 1 for an overview of the different conditions).

Overall structure of the experiment. Participants completed a 30-minute practice task, during which they familiarized themselves with the described tasks and learned all the cues (control: “middle blue”; updating: “2-back”; inhibition: “double yellow”; updating & inhibition: “double yellow 2-back”). Participants who did not reach criterion of 66% accuracy in each of the conditions ($n = 2$), were debriefed, thanked and compensated for their participation and did not continue to the scanning phase of the study.

The overall experimental paradigm was structured such that there were 12 trials (1 task switch trial and 11 “process pure” trials) per block, 12 blocks per run (3 blocks of each of the 4 conditions listed above) and 4 runs per session. There were a total of 12 blocks of each condition throughout a testing session. This summed to 132 trials of each condition, with the exception of task switching, which totalled 48 trials. The experiment was designed to have a 1:1 ratio of correct yes:no responses, and a 1:1:1 ratio of correct yes:no:withhold responses in conditions where the “double yellow” rule was in effect (in the inhibition and combined inhibition & updating conditions). In other words, the participant was expected to withhold his/her response on a third of trials during the inhibition and the combined updating & inhibition conditions (44 withhold trials/condition) (see Table 1 for a summary of the number of trials). The order of the blocks was pseudo-randomized for every participant, ensuring that the same condition was not presented back-to-back (to keep the task switch trials valid).

We also included null trials to jitter all the events. Using the equation of $1/(N + 1)$, (where N = the number of trial types) to determine the optimal number of null trials to include in our design (Friston, Zarahn, Josephs, Henson, & Dale, 1999). Given that we

had two types of trials in the control and updating conditions (correct “yes” and “no” responses) and three types of trials in the inhibition and combined conditions (correct “yes,” “no,” and “withhold” responses) (see Table 1), we dedicated a third of total scan time to null trials (to err on the side of more null trials). Null trials were randomly distributed between all trials, lasting between 2–6 seconds. In addition, the experimental runs were preceded and followed by 30 seconds of baseline rest, where the participants were simply looking at a fixation cross (see Figure 2 for run layout).

MRI Data Acquisition and Pre-Processing

Participants were scanned using a Siemens 3T Magnetom Tim Trio MRI scanner at York University. Visual stimuli were back-projected on to a screen that the participants viewed through a mirror. Functional scans were acquired using a 32-channel head coil. We used a T2*-weighted 2D EPI sequence sensitive to BOLD contrast, acquired in the oblique-axial plane (36 axial slices, 3mm iso, repetition time = 2000ms, echo time = 30ms, flip angle = 90°, field of view = 240mm² with a 80 x 80 matrix size). High-resolution 3D structural images were acquired using a T1-weighted sequence, multi-planar rapid gradient echo (MP-RAGE) (192 slices, 1mm iso, repetition time = 1900ms, echo time = 2.5ms, TI = 900, flip angle = 9°, field of view = 256mm².)

For each of the 4 functional runs, 264 scans were collected. All pre-processing was accomplished using an in-house pre-processing pipeline based on AFNI (Cox, 1996). We generated physiological noise regressors and regressed out noise due to respiration and heart rate. Each run was corrected for slice-time dependent offsets. We then motion-corrected each subject to the 8th TR of the first run of the session. We created whole-brain masks and co-registered to the MP-RAGE anatomical image. We

detrended each voxel's time series against Legendre polynomials up to the 4th order and estimated head motion parameters to account for scanner drift and participant movement. The data were smoothed within the whole-brain mask using a Gaussian kernel of full-width, half-maximum of 6mm. Finally, we used a linear registration to transform all the data to Montreal Neurological Institute (MNI) coordinates.

Data Analysis

We carried out our analysis of the fMRI data using Partial Least Squares (PLS, Krishnan et al., 2011) to identify patterns of brain activity associated with each executive control condition. PLS is a multivariate statistical approach used for the analysis of complex datasets, including neuroimaging data. It is a data-driven approach that creates a data matrix using the experimental model (with all its experimental conditions), the event onset times, and the intensity of each voxel at each time point. Singular value decomposition is conducted on the matrix to identify significant patterns of activation, or latent variables (LVs) in the data. LVs are composed of two vectors, one representing the components of the experimental design that account for the most variance in voxel activation, and the other representing the spatiotemporal pattern in the brain that best represents these variances (Krishnan et al., 2011; McIntosh, Chau, & Protzner, 2004). Put another way, LVs express the covariance between brain voxels and experimental design. Significant LVs can be interpreted as the patterns of BOLD activity across the whole brain that are best explained by the experimental design.

The statistical significance of each LV is determined by permutation testing (500 permutations). Each brain voxel has a weight, known as a salience, which indicates how strongly that voxel contributes to the LV overall; the reliability of the brain saliences is

determined by bootstrap resampling (300 bootstraps). The extent to which each participant expresses each LV (“brain score”) was calculated by multiplying each voxel’s salience by the BOLD signal in the voxel, and summing over all brain voxels for each participant for each condition. The average brain scores across all participants for each condition in each LV were calculated, as were their associated 95% confidence intervals, using the bootstrap analysis.

Results

One participant was excluded from the analysis due to poor performance (scoring less than chance on one or more of the three main executive control tasks). This left 22 participants included in the final analysis (11 women, 11 men, $M_{\text{age}} = 22.14$, age range: 18–28 years), two of which were left-handed. We analyzed the data with and without the left-handed participants, and found no difference in the structure of the LVs, and the corresponding patterns of brain activity were similar upon visual inspection. Therefore, we have included their data in the analyses below to maintain higher statistical power.

Behavioural Results

We analyzed participants’ accuracy (percent correct trials) and mean reaction times (RT) for correct trials for each condition (see Table 2) using one-way repeated-measures ANOVAs to assess behavioural performance. We report the accuracy for both the inhibition condition overall (all the trials in the “double yellow” blocks, including non-inhibition trials) and inhibition events (specific instances when participants were required to withhold their response during the inhibition block). However, the data from the inhibition condition as a whole were included in our behavioural statistical analysis.

Accuracy. Differences between participants' performance on the different conditions were assessed using a one-way repeated-measures ANOVA. The repeated factor was condition and the dependent variable was percent accuracy. First, we ran Mauchly's test of sphericity on the data to assess whether carrying out a standard F -test was appropriate. We found evidence that our data may not meet the assumption of sphericity ($\chi^2(9) = 49.34, p < .01$, Greenhouse-Geisser $\epsilon = .48$, Huynh-Feldt $\epsilon = .53$) Therefore, we applied a Greenhouse-Geisser correction to our degrees of freedom when considering the statistical significance of the F -test. The ANOVA indicated a significant effect of condition ($F(1.93, 40.56) = 35.24, p < .01$, partial $\eta^2 = .63$).

Follow-up pairwise comparisons (using a Bonferroni correction for multiple comparisons, $p = 0.005$) found that there were no significant differences between performance on the three individual executive control conditions (updating vs. inhibition: $p = .01$, updating vs. task switch: $p = .05$, inhibition vs. task switch: $p = .42$). In other words, the differences between participants' accuracy on the three executive control conditions did not survive a Bonferroni correction. However, accuracy on all other conditions was significantly different from each other; performance on the control condition was significantly higher than all other conditions and performance on the combined updating and inhibition condition was significantly lower than all other conditions (see Table 3).

Using Shapiro-Wilk tests, we found evidence that the assumption of normality was violated in the control ($W(22) = .90, p = .03$), updating ($W(22) = .90, p = .04$), and task switching ($W(22) = .80, p = .00$) conditions. A visual inspection of the frequency distribution revealed that the data for these conditions was negatively skewed, typical of

ceiling effects. The assumption of normality is often violated in samples of less than 30 participants, so we confirmed the findings above using nonparametric tests. We ran a Friedman test to evaluate difference in medians among participants' accuracy for each condition. This test was also significant ($\chi^2(4) = 59.99, p < .01$) and the Kendall coefficient of concordance of .68 indicated strong differences among the five conditions. Follow-up pairwise comparisons were conducted using Wilcoxon tests and controlling for Type I errors using a Bonferroni correction ($p = .005$). We found the same pattern of results – there was no difference between updating, inhibition and task switching, but all other comparisons were statistically significant (see supplementary tables for additional details on this analysis).

Reaction time. A one-way repeated-measures ANOVA was conducted, with condition as the repeated factor and mean RT as the dependent variable. We found no evidence that that we were sampling from a non-normal distribution for any condition (Shapiro-Wilk tests were all non-significant); however, we once again found evidence that our data did not meet the assumption of sphericity (Mauchly's $\chi^2(9) = 38.20, p < .01$, Greenhouse-Geisser $\epsilon = .59$, Huynh-Feldt $\epsilon = .67$). Therefore, we applied a Greenhouse-Geisser correction to our degrees of freedom when assessing the statistical significance of the *F-test*. The results of the ANOVA indicated a significant effect of condition on RT ($F(2.36, 49.58) = 25.83, p < .01, \eta^2 .55$). Follow-up pairwise comparisons revealed that RTs were significantly different across all conditions (at the corrected alpha value of .005) with the exception of control vs. updating, inhibition vs. the combined condition, and task switching vs. the combined condition. For the three individual executive control conditions, the patterns of RTs were as follows: updating < inhibition ($p < .001$), updating

< task switching ($p < .001$), inhibition < task switching ($p = .002$) (see Table 4 for all comparisons and associated statistics).

We also carried out the same analysis of participants' median RT, in case the individual participants' RTs were not normally distributed. The findings were almost identical ($F(2.58, 54.25) = 29.66, p < .01, \text{partial } \eta^2 = .59$). The only finding that differed from the analysis of average RT was the pairwise test between control and updating, which was now significant (see supplementary tables for analysis of Median RT).

Neuroimaging Results

Using event-related mean-centered PLS, we carried out four analyses of the fMRI data. We analyzed the pattern of activation that emerged related to all conditions in one analysis (full model analysis) and then each of the executive processes of interest (updating, inhibition and task switching) individually against the control condition. We found significant LVs in each of the four analyses. All analyses were carried out for correct trials only. For the inhibition condition, we only considered events where the participants correctly withheld their response. We report results from “lag 2,” approximately 4s after event onset. In selecting this lag value, we attempted to balance the typical timing of the hemodynamic response function's peak (4–6s) with the potential contamination of subsequent trials (at 4s, there is a maximum of only one intervening trial). Patterns of brain activation for all lags are shown in our supplementary figures. Cluster size thresholds were set to a maximum of 1000 voxels to identify dissociable activation peaks within very large clusters. Finally, we created a conjunction map of the individual executive process analyses to contrast the whole-brain pattern of activation of each executive process and define domain-general areas of activation. Each individual

analysis included in the conjunction was created using a bootstrap ratio (BSR) of ± 2.5 ($p < .0124$); all voxels that survived this threshold were included.

Full-model analysis. The full model analysis revealed two significant LVs. The first LV ($p < .001$) accounted for 82.45% of the covariance in the data and dissociated task switching from all other task conditions (see Figure 3). The network of task switching activity included the precuneus and the superior parietal lobes bilaterally, as well as the left middle gyrus/dorsolateral pre-frontal cortex (DLPFC) and left prefrontal gyrus. This pattern of activation also included the posterior cingulate gyrus and superior medial PFC, including the supplementary motor area (SMA) and pre-SMA. We also found activity in the primary visual cortex (see Table 5 for coordinates).

The second significant LV ($p = .012$) accounted for 11.51% of the covariance in the data and was driven by the dissociation of the inhibition condition from all other conditions (see Figure 4). The most striking in the pattern of activation is the left motor cortex activity related to the non-inhibition conditions. However, there were also areas positively associated with the inhibition trials. They included the bilateral anterior inferior and middle frontal gyri, the superior medial frontal gyrus, near the pre-SMA, and the fusiform/middle temporal gyrus (see Table 5 for coordinates).

Individual updating analysis. Next, we ran another event-related mean-centered PLS analysis considering only correct control trials and correct updating trials. This analysis yielded a significant LV ($p = .004$) accounting for 100% of the covariance in the data (see Figure 5). The updating-related network of activation was mostly right lateralized, with activity in the right anterior PFC, right caudate and right superior parietal

lobule. Bilaterally, we found activity in the insula, DLPFC, medial PFC and inferior parietal lobule (see Table 6 for coordinates).

Individual inhibition analysis. We also ran an analysis considering only correct control trials and trials on which participants correctly withheld their responses in the “double yellow” condition. We found a significant LV ($p = .030$) accounting for 100% of the covariance in the data (see Figure 6). The pattern of inhibition-related activity was confined to the PFC, including the right inferior frontal gyrus, right superior frontal gyrus, as well as the bilateral middle frontal gyri and medial frontal gyrus (see Table 7 for coordinates).

Individual task switch analysis. Finally, we ran an analysis considering only correct control trials and correct task switch trials. We found a significant LV ($p < .001$) accounting for 100% of the covariance in the data (see Figure 7). The task-switching related network included the bilateral superior parietal lobules and precuneus, left middle and precentral gyri, left cingulate cortex and right superior frontal gyrus (see Table 8 for coordinates).

Conjunction of individual analyses. The last three analyses (control & updating, control & inhibition, and control & task switch) were used to create a conjunction map of the results. The executive process-related patterns of activation from each analysis were overlaid onto a single image to contrast the different networks and identify areas of conjunction (Figure 8). Control-related activations were not included. We found no point where all three executive processes overlapped. However, all three conditions were associated with activity in the left anterior inferior frontal gyrus.

Discussion

In this study, we examined the neural correlates of three proposed component processes of executive function. Using a novel paradigm, we were able to study updating, inhibition and task switching in a standardized, within-subject design. Applying a data-driven multivariate approach to analyzing our data enabled us to identify whole-brain patterns of activity that were reliably associated with each executive process included in our experimental design. When considering the full experimental model, two reliable patterns emerged. The first was driven by the effect of task switching in contrast to all other conditions. The second was related to inhibition dissociating from all other conditions. Follow-up analyses of each individual executive task, considered only with the control condition, revealed three distinctive networks associated with each of the executive processes of interest. These condition-wise results aligned with previous studies of specific control processes, but also differed in particular core respects. While our findings provide support for a fractionated model of executive functioning at the level of the brain, these data may also be in line with alternate models of executive control.

Full-Model

The results of the full-model analysis, including all task conditions, revealed partial support for the fractionation model of executive functioning (Miyake, Friedman, Emerson, Witzki, Howerter, & Wager, 2000). Two significant patterns emerged dissociating task switching and inhibition from all other conditions, which supports the dissociation of executive functioning into component processes. Though non-executive processes were also likely associated with the pattern of brain activity identified in the full-model analysis (more on this below), the findings are compatible with previous neuroimaging literature

on task switching and inhibition. The first pattern, which dissociated task switching from all other conditions (Figure 3, Table 5), included task-switching-related activity in the superior parietal lobule bilaterally, medial PFC and lateral PFC (including the inferior frontal junction - IFJ) typical of task-switching activity, as previously reported in meta-analytic reviews of the switching literature (e.g., Derrfuss, Brass, Neumann & von Cramon, 2005; Kim, Cilles, Johnson, & Gold, 2012; Wager, Jonides & Reading 2004). The second pattern differentiated inhibition-related activation from all other conditions (Figure 4, Table 5). Task-related activity during inhibition trials was observed in cortical regions identified in the literature as critical nodes for response inhibition, including the right inferior frontal gyrus (IFG) and pre-SMA (for reviews, see: Aron, 2007; Chambers, Garavan & Bellgrove, 2009; Mostofsky & Simmonds, 2008).

While these results are consistent with a fractionation account, the updating condition was not associated with a dissociable pattern of brain activity in the full-model analysis. This may be due to the constant working memory demands inherent in the present study. To successfully complete the tasks, participants were required to continuously remember which rules they were currently following and which rules were associated with each cue screen presented to them. This created a continuous working memory load throughout the experiment, which may have obscured the effect of the updating condition in the analysis of all conditions.

Nonetheless, alternate interpretations of the current findings are possible. The current protocol was designed to investigate a three-factor model of executive functioning as suggested in the original work by Miyake and colleagues (Miyake et al., 2000). However, this model has recently been updated (Miyake & Friedman, 2012). In this

revised fractionation account, inhibition is considered to be a common process underlying executive functioning, while updating and shifting are considered to be dissociable subcomponents. Specifically, inhibition was perfectly correlated with the common executive function variable in their factor analyses of behavioural performance of executive functioning tasks. Therefore, rather than considering inhibition as a component process of overall executive functioning, is it incorporated under the domain-general ability to maintain goals and use goal-related information to guide decision making. In contrast, updating and shifting are considered dissociable executive functions that represent domain-specific abilities. If the updated Miyake and Friedman (2012) model holds true at the level of the brain, we might have expected to see a task-switching-related LV and an updating-related pattern of brain activity in our full-model analysis (with inhibition-related variance common to both). Though we did find a task-switching pattern, we found no updating-related pattern of activity in our full-model analysis. However, the authors suggest that shifting may display an opposing pattern of behavioural correlation than the common/inhibition executive function, meaning that performance on shifting tasks may be negatively related to performance on executive function tasks in general. This would be consistent with the first activation pattern that emerged from our full model analysis (Figure 3, Table 5).

Another model of executive control functioning suggests that task switching (or cognitive flexibility) relies on inhibitory control and working memory (Diamond, 2013). If this is the case, patterns of activity related to inhibition and updating may not have emerged from the full-model analysis because the task-switching condition may have accounted for the model variance associated with all three executive control processes.

Indeed, the task switching pattern accounted for 82.45% of the variance in our full model. However, the results of the condition-wise analyses, reviewed below, did not reveal substantive overlap between the task-switching pattern of activation and the patterns of activation related to inhibition and updating, suggesting that our data are not fully convergent with this model.

Despite careful efforts to match our conditions on all factors of non-interest, there remain condition-specific differences that may have contributed to the findings when all conditions are contrasted in a full experimental model. Task switching was associated with greater activity in the primary visual cortex (cuneus and calcarine fissure - Figure 3). This pattern of brain response may reflect the trial structure for the task switch condition. Switch trials occurred immediately after the visual cue indicating the upcoming task. While the trial structure was jittered to allow the switch cue and switch trials to be modeled independently, these events may not have been fully dissociated in our task design (however, it is important to note that activity in the visual cortex is consistent with previous literature on tasks switching: Buchsbaum, Greer, Chang, & Berman, 2005; Kim et al., 2012; Wager et al., 2004). Moreover, brain activity for the switch condition was mostly left lateralized, suggesting that language-based cueing may have contributed to this pattern of brain activation.

The other significant pattern of activation that emerged from our full-model analysis contrasted correct inhibition trials against all other conditions. The majority of the brain activity in this LV was related to the non-inhibition conditions (Figure 4, Table 5). The largest and most reliable cluster of non-inhibition activity was found in the left motor cortex. This is consistent with the fact that correct inhibit trials required participants to

withhold their response, while in all other conditions correct trials required participants to make a response in the form of a right-handed button press. This being the case, it is possible that this pattern was driven in large part by the difference in motor demands between the inhibition condition and the other tasks, rather than by the unique cognitive demands of withholding a pre-potent response.

Taken together, one might argue that the three executive control processes under study rely on a common set of brain regions, and the only reliable neural differences associated with each were the subtle differences in trial structure between the conditions. It might be the case that the full-model analysis represents a task switching pattern, related to the unique perceptual or linguistic characteristics of the task switch trials, and a second inhibition pattern, related to a simple difference in motor demands of inhibition and non-inhibition tasks. This would imply that the different conditions included in the present study did not dissociate on the basis of their cognitive demands. If this interpretation is correct, it would support the idea that different executive control processes rely on a common neural network. Several investigators endorse this view (e.g., Braver, Paxton, Locke & Barch, 2009, Duncan & Owen, 2000; Duncan et al., 2000; & Niendam et al., 2012). Indeed, there is evidence in keeping with a more unitary view of executive functioning, where the most complex cognitive tasks rely on a common frontoparietal network including the lateral PFC, dorsal anterior cingulate cortex (ACC) and the posterior parietal lobes. On the other hand, were executive control a unitary construct, we might expect to find a pattern of activation related to executive processes overall (dissociating the control conditions from the executive tasks). However, no such pattern emerged in the current study.

Individual Executive Processes

To address the potential condition-wise differences in trial-structure, we conducted individual analyses of each executive control process contrasted with a tightly matched (non-executive) control condition. These results provide strong support for the fractionation hypothesis. When analyzed with control trials only, each executive process was associated with a clearly dissociable pattern of whole-brain activation. A conjunction map of the three analyses revealed that there was not a single point where all three executive functions overlapped (though areas of activity related to all three of the executive control processes bordered each other in the left anterior IFG) (see Figure 8). Below we review each of the condition-specific analyses.

Updating. The updating-related activity seen in this analysis included the medial superior PFC/dorsal ACC, the precuneus, the bilateral ventrolateral PFC (VLPFC), the bilateral DLPFC, the bilateral insula, and the bilateral inferior parietal lobule (IPL). Additionally, there was right-sided activity in the frontal pole, superior parietal lobule and caudate nucleus (see Figure 5, Table 6). This profile of activity is typical of n-back tasks (for meta-analysis of n-back tasks, see Owen, McMillan, Laird & Bullmore, 2005). We note that the updating task included in the current study was not a classic match-to-sample n-back task, but rather a delayed response. Though this may require less manipulation of the information kept in working memory by the participants, they must nonetheless continuously update the information stored in working memory and select the correct information from multiple items active in working memory. For this reason, we maintain that the updating condition represents an executive attention challenge similar to a classic n-back task (Petrides, Alivisatos, Meyer, & Evans, 1993, also argue that

active maintenance recruits the same brain areas as other working memory tasks). Whereas Owen et al.'s (2005) findings showed a largely bilateral activation pattern, our current analysis showed greater recruitment of the right hemisphere. In their meta-analysis of working memory tasks, Wager and Smith (2003) point out that an increase in executive demands of a working memory task increased the right lateralization of activity within the PFC. To successfully carry out the updating task in the current study, participants were required to keep in mind which task they were currently performing in addition to previous trial information. These additional executive demands may be the reason why we found greater activity in the right hemisphere. Wager and Smith (2003) also found that the DLPFC and the superior frontal sulcus (centered around the pre-motor cortex) are preferentially recruited in continuous updating tasks, which is consistent with our findings.

Moreover, the brain regions associated with updating in our condition-wise analysis closely map onto the domain-general “frontoparietal control network” (Vincent, Kahn, Snyder, Raichle, & Buckner, 2008). This control network overlaps with networks associated with general intelligence (Duncan et al., 2000). Indeed, Friedman et al. (2006) found that updating was the only executive control process correlated with measures of intelligence. If working memory relies on a domain-general neural network, this may be why an updating-related pattern of activation did not emerge in our full-model analysis.

Inhibition. The findings from the individual inhibition analysis closely overlapped with the second significant pattern of activation from the full-model analysis. Inhibition-related activity was observed in bilateral VLPFC (particularly near the frontal pole), right superior frontal gyrus/DLPFC and in the medial superior frontal gyrus/pre-SMA (see

Figure 6, Table 7). Buchsbaum and colleagues (2005) carried out a meta-analysis of experiments involving commonly used Go/No-Go tests of inhibition and found several regions of common activation across studies that corresponded closely to the current findings. Namely, they found active clusters related to inhibition performance in the bilateral IFG, bilateral Middle Frontal Gyrus (MFG), right superior frontal gyrus and medial frontal gyrus. Though the current findings include bilateral IFG activation, most of the neuroimaging literature on inhibitory processes has selectively implicated right IFG (e.g., Garavan, Ross, & Stein, 1999; Konishi et al., 1999; Rubia, Smith, Brammer, & Taylor, 2003; for review, see Aron, Robbins, & Poldrack, 2004). Aron and colleagues (2004) did report evidence that recruitment of the left IFG may be related to inhibition and interference resolution in working memory paradigms, similar to the current study (e.g., Jonides, Smith, Marshuetz, Koeppe, & Reuter-Lorenz, 1998). Another brain region often associated with response inhibition is the pre-SMA (Chambers et al., 2009, Mostofsky & Simmonds, 2008; Simmond, Pekar, & Mostofsky, 2008), which we also found.

Task switching. Our individual analysis of task switching yielded a similar pattern of activation as the first pattern that emerged in the full-model analysis (Figure 7, Table 8). Switching-related activity was widespread, with large clusters of activation in the parietal lobes bilaterally (including the precuneus, superior parietal lobule and the angular gyrus), the posterior cingulate cortex, medial superior PFC, left MFG/DLPFC, and left precentral gyrus (thalamic and middle temporal gyrus activity were also detected at slightly lower thresholds). Our findings are consistent with most existing neuroimaging studies of task switching, which reliably report lateral PFC and superior/posterior parietal activity, irrespective of study design (Braver, Reynold & Donaldson, 2003; Buchsbaum et

al., 2005; DiGirolamo et al., 2001; Dove, Pollmann, Schubert, Wiggins, & von Cramon, 2000; Dreher, Koechlin, Ali, & Grafman, 2002; Kim et al., 2012; Kimberg, Aguirre, & D'Esposito, 2000; Ravizza & Carter, 2008; Sohn, Ursu, Anderson, Stenger, & Carter, 2000; Wager et al., 2004). Several of these studies also observe greater left-lateralization of task-switching activity (e.g., Braver et al., 2003; Kim et al., 2012; Ravizza & Carter, 2008). Braver et al., (2003) argue that left lateralization of task switching activity reflects the semantic classification of the tasks when a switch takes place. Many authors agree that the DLPFC activity seen during task switching is related to the maintenance of task-set and task-related goals, particularly in the presence of working memory demands (Braver et al., 2003; Kim et al., 2012; Ruge, Jamadar, Zimmermann & Karayanidis, 2013), while parietal activity is related to reallocation of attention to the new task (Braver et al., 2003; Ruge et al., 2013). This proposed neuroanatomical functions fit with Ravizza & Carter's (2008) findings that DLPFC is preferentially recruited during rule switching, whereas the superior parietal lobule is preferentially recruited during perceptual shifting. Our behavioural findings are also in keeping with the established literature, as we find a behavioural switch cost, as seen by longer reaction time on task-switch trials (see Monsell, 2003 for review of the behavioural literature). Although our findings are compatible with the majority of the task switching literature, we did not find task switching-related insular activity, despite the fact that some, but not all, researchers have identified it as a critical hub for switching between networks and tasks (e.g., Buchsbaum et al., 2005; Kim et al., 2012; Menon & Uddin, 2010; Wager et al., 2004).

Conjunction analysis. As may be observed from Figure 8, the conjunction analysis reveals relatively sparse overlap amongst the three condition-wise analyses.

Although the three executive control processes studied in this experiment are widely recognized as components of executive functioning (Diamond, 2013; Lehto, Juujärvi, Kooistra, & Pulkkinen, 2003; Miyake et al., 2000), we found no point of activation common to all three processes, consistent with the fractionation model. However, there were areas common to two of the three processes studied here. Regions of overlap between the task switching condition and the updating condition are similar to those found by Wager et al. (2004) in their conjunction analysis between task switching and working memory tasks (specifically, medial superior PFC, right premotor cortex and IPL). Some of these areas (such as medial superior PFC and IPL) also overlap with nodes of the frontoparietal control network (described above) and so may represent domain-general regions of executive control in the brain. Furthermore, although there was no point of overlap between all three conditions, there was a region in the left anterior inferior frontal gyrus, in the frontal pole, where the three processes nearly overlap. The anterior inferior frontal gyrus is interesting bilaterally, as it is an area of overlap between task switching and inhibition on the left and updating and inhibition on the right (see Figure 8). This finding may be in line with the gateway hypothesis of frontal pole function put forth by Burgess, Dumontheil, and Gilbert (2007), which proposes that the rostral PFC is the seat of a *supervisory attentional gateway* mediating attention between external and internal information in the brain. Nonetheless, when taken together, these findings provide strong support for the overall dissociation of the neural substrates underlying sub-components of executive control.

Study Limitations

As noted earlier, one of the limitations of the study was the constant working

memory load associated with remembering which rule to apply on all trials. It is possible that this created a confound, which potentially prevented us from uncovering more robust updating-related activity in the full-model analysis. Indeed, increased working memory demands have been shown to alter the neural activity profile of an inhibition task (Simmonds et al., 2008). Another possible limitation of the current study was the absence of control trials for the task-switch condition. These would be trials preceded by a cue-screen, but would not require the participants to switch tasks. However, the inclusion of an additional condition would have reduced trials for the core conditions of interest, thereby reducing statistical power. We instead opted to address this by inserting a jitter into the trial design that allowed us to independently model switch trials vis-à-vis the cue presentation. Although motor demands were controlled across conditions for the most part, we were unable to control for the absence of a motor response on inhibition trials. In future studies investigating inhibitory processes, it will be necessary to clearly dissociate the absence of a motor response from the upstream cognitive components of inhibition.

Future Directions

The current investigation provides a necessary foundation to examine how the neural profile of different executive control processes is altered across the adult lifespan. This would extend the work carried out by Turner & Spreng (2012) examining the differences in the neural underpinning inhibition and working memory in both healthy younger and older adults. In their meta-analysis of previous literature, they found that age-related changes in the neural networks recruited during executive functioning vary according to which specific executive function is assessed (Turner & Spreng, 2012). Carrying out the present study with an older adult population would provide a direct

empirical test of these conclusions. Moreover, it would elucidate the profile of task switching-related processes across the lifespan, as this executive control process was not included in the original meta-analysis.

Another exciting horizon for neurocognitive research is the study of the different temporal components of executive control processes. Comparing the sustained and transient patterns of activation associated with each process may yield valuable insight into the complex nature of executive control in the brain. Using a mixed block/event-related analysis (Braver & Barch, 2006; Donaldson, Petersen, Ollinger, & Buckner, 2001; Dosenbach et al., 2006) would enable us to capture both the overall “brain state” associated with each process, as well as the trial-by-trial, response-related activity. Using this approach, we would be able to dissociate the activity related to the task-switch cue, the instantiation of the new task, in addition to the maintenance of the new task set. This type of exploration is critical since the dissociation of function at the level of the brain may not only take place at an anatomical level, but also at a temporal level (Braver, Paxton, Locke & Barch, 2009).

Conclusion

In conclusion, the present study represents the first investigation of the neural basis of executive control processes using a within-subject design and a single task paradigm. We found compelling evidence that updating, inhibition and task switching are subserved by different patterns of brain activity. These patterns were largely dissociable, with updating recruiting regions of the frontoparietal control network, task switching recruiting a mostly left lateralized network comprised of lateral PFC and posterior parietal cortex, and inhibition recruiting specific areas within VLPFC and pre-SMA. Our analysis

of all conditions yielded partial support for the fractionation of executive control at the level of the brain, while our individual analyses of each executive process of interest showed clearly distinct patterns of activity. Thus, the preponderance of evidence in the current investigation supported the hypothesis that the neural correlates of executive control are dissociable. This signifies an important step in developing a clearer and more concise understanding of the organization of executive functioning in the human brain and lays the groundwork for examinations of the neural basis of executive control functions in aging and brain disease.

References

- Alvarez, J. A., & Emory, E. (2006). Executive function and the frontal lobes: A meta-analytic review. *Neuropsychology Review*, *16*(1), 17-42. doi:10.1007/s11065-006-9002-x
- Aron, A. R. (2007). The neural basis of inhibition in cognitive control. *The Neuroscientist*, *13*(3), 214-228. doi:10.1177/1073858407299288
- Aron, A. R., Robbins, T. W., & Poldrack, R. A. (2004). Inhibition and the right inferior frontal cortex. *Trends in Cognitive Sciences*, *8*(4), 170-177. doi:10.1016/j.tics.2004.02.010
- Baddeley, A. (1992). Working memory. *Science*, *255*(5044), 556-559. doi:10.1126/science.1736359
- Braver, T. S., & Barch, D. M. (2006). Extracting core components of cognitive control. *Trends in Cognitive Sciences*, *10*(12), 529-532. doi:10.1016/j.tics.2006.10.006
- Braver, T. S., Paxton, J. L., Locke, H. S., & Barch, D. M. (2009). Flexible neural mechanisms of cognitive control within human prefrontal cortex. *Proceedings of the National Academy of Sciences*, *106*(18), 7351-7356. doi:10.1073/pnas.0808187106
- Braver, T. S., Reynolds, J. R., & Donaldson, D. I. (2003). Neural mechanisms of transient and sustained cognitive control during task switching. *Neuron*, *39*(4), 713-726. doi:10.1016/S0896-6273(03)00466-5

- Buchsbaum, B. R., Greer, S., Chang, W. L., & Berman, K. F. (2005). Meta-analysis of neuroimaging studies of the Wisconsin Card-Sorting task and component processes. *Human Brain Mapping, 25*(1), 35-45. doi:10.1002/hbm.20128
- Burgess, P. W., Dumontheil, I., & Gilbert, S. J. (2007). The gateway hypothesis of rostral prefrontal cortex (area 10) function. *Trends in cognitive sciences, 11*(7), 290-298. doi:10.1016/j.tics.2007.05.00
- Chambers, C. D., Garavan, H., & Bellgrove, M. A. (2009). Insights into the neural basis of response inhibition from cognitive and clinical neuroscience. *Neuroscience & Biobehavioral Reviews, 33*(5), 631-646. doi:10.1016/j.neubiorev.2008.08.016
- Cox, R. W. (1996). AFNI: software for analysis and visualization of functional magnetic resonance neuroimages. *Computers and Biomedical research, 29*(3), 162-173. doi:10.1006/cbmr.1996.0014
- D'Esposito, M., Postle, B. R., & Rypma, B. (2000). Prefrontal cortical contributions to working memory: Evidence from event-related fMRI studies. *Experimental Brain Research, 133*(1), 3-11. doi:10.1007/s002210000395
- Derrfuss, J., Brass, M., Neumann, J., & Von Cramon, D. Y. (2005). Involvement of the inferior frontal junction in cognitive control: Meta-analyses of switching and Stroop studies. *Human Brain Mapping, 25*(1), 22-34. doi:10.1002/hbm.20127
- Diamond, A. (2013). Executive functions. *Annual review of psychology, 64*, 135-168. doi:10.1146/annurev-psych-113011-143750
- DiGirolamo, G. J., Kramer, A. F., Barad, V., Cepeda, N. J., Weissman, D. H., Milham, M. P., ... & McAuley, E. (2001). General and task-specific frontal lobe recruitment in older adults during executive processes: A fMRI investigation of task-

- switching. *Neuroreport*, 12(9), 2065-2071. doi:10.1097/00001756-200107030-00054
- Donaldson, D. I., Petersen, S. E., Ollinger, J. M., & Buckner, R. L. (2001). Dissociating state and item components of recognition memory using fMRI. *Neuroimage*, 13(1), 129-142. doi:10.1006/nimg.2000.0664
- Dosenbach, N. U., Fair, D. A., Miezin, F. M., Cohen, A. L., Wenger, K. K., Dosenbach, R. A., ... & Petersen, S. E. (2007). Distinct brain networks for adaptive and stable task control in humans. *Proceedings of the National Academy of Sciences*, 104(26), 11073-11078. doi:10.1073/pnas.0704320104
- Dosenbach, N. U., Visscher, K. M., Palmer, E. D., Miezin, F. M., Wenger, K. K., Kang, H. C., ... & Petersen, S. E. (2006). A core system for the implementation of task sets. *Neuron*, 50(5), 799-812. doi:10.1016/j.neuron.2006.04.031
- Dove, A., Pollmann, S., Schubert, T., Wiggins, C. J., & Yves von Cramon, D. (2000). Prefrontal cortex activation in task switching: an event-related fMRI study. *Cognitive Brain Research*, 9(1), 103-109. doi:10.1016/S0926-6410(99)00029-4
- Dreher, J. C., Koechlin, E., Ali, S. O., & Grafman, J. (2002). The roles of timing and task order during task switching. *Neuroimage*, 17(1), 95-109. doi:10.1006/nimg.2002.1169
- Duncan, J., Seitz, R. J., Kolodny, J., Bor, D., Herzog, H., Ahmed, A., ... & Emslie, H. (2000). A neural basis for general intelligence. *Science*, 289(5478), 457-460. doi:10.1126/science.289.5478.45

- Duncan, J., & Owen, A. M. (2000). Common regions of the human frontal lobe recruited by diverse cognitive demands. *Trends in Neurosciences*, 23(10), 475-483. doi:10.1016/S0166-2236(00)01633-7
- Friedman, N. P., Miyake, A., Corley, R. P., Young, S. E., DeFries, J. C., & Hewitt, J. K. (2006). Not all executive functions are related to intelligence. *Psychological Science*, 17(2), 172-179. doi:10.1111/j.1467-9280.2006.01681.x
- Friedman, N. P., & Miyake, A. (2004). The relations among inhibition and interference control functions: a latent-variable analysis. *Journal of Experimental Psychology: General*, 133(1), 101-135. doi:10.1037/0096-3445.133.1.101
- Friston, K. J., Zarahn, E. O. R. N. A., Josephs, O., Henson, R. N. A., & Dale, A. M. (1999). Stochastic designs in event-related fMRI. *Neuroimage*, 10(5), 607-619. doi:10.1006/nimg.1999.0498
- Miyake, A., & Friedman, N. P. (2012). The nature and organization of individual differences in executive functions four general conclusions. *Current Directions in Psychological Science*, 21(1), 8-14. doi:10.1177/0963721411429458
- Garavan, H., Ross, T. J., & Stein, E. A. (1999). Right hemispheric dominance of inhibitory control: an event-related functional MRI study. *Proceedings of the National Academy of Sciences*, 96(14), 8301-8306. doi:10.1073/pnas.96.14.8301
- Hanania, R., & Smith, L. B. (2010). Selective attention and attention switching: towards a unified developmental approach. *Developmental Science*, 13(4), 622-635. doi:10.1111/j.1467-7687.2009.00921.x

- Hasher, L., & Zacks, R. T. (1988). Working memory, comprehension, and aging: A review and a new view. *Psychology of Learning and Motivation*, 22, 193-225. doi:10.1016/S0079-7421(08)60041-9
- Jonides, J., Smith, E. E., Marshuetz, C., Koeppe, R. A., & Reuter-Lorenz, P. A. (1998). Inhibition in verbal working memory revealed by brain activation. *Proceedings of the National Academy of Sciences*, 95(14), 8410-8413. doi:10.1073/pnas.95.14.8410
- Kim, C., Cilles, S. E., Johnson, N. F., & Gold, B. T. (2012). Domain general and domain preferential brain regions associated with different types of task switching: A Meta-Analysis. *Human Brain Mapping*, 33(1), 130-142. doi:10.1002/hbm.21199
- Kimberg, D. Y., Aguirre, G. K., & D'Esposito, M. (2000). Modulation of task-related neural activity in task-switching: An fMRI study. *Cognitive Brain Research*, 10(1), 189-196. doi: 10.1016/S0926-6410(00)00016-1
- Konishi, S., Nakajima, K., Uchida, I., Kikyo, H., Kameyama, M., & Miyashita, Y. (1999). Common inhibitory mechanism in human inferior prefrontal cortex revealed by event-related functional MRI. *Brain*, 122(5), 981-991. doi:10.1093/brain/122.5.981
- Krishnan, A., Williams, L. J., McIntosh, A. R., & Abdi, H. (2011). Partial Least Squares (PLS) methods for neuroimaging: A tutorial and review. *Neuroimage*, 56(2), 455-475. doi:10.1016/j.neuroimage.2010.07.034
- Lehto, J. E., Juujärvi, P., Kooistra, L., & Pulkkinen, L. (2003). Dimensions of executive functioning: Evidence from children. *British Journal of Developmental Psychology*, 21(1), 59-80. doi:10.1348/026151003321164627

- Lemire-Rodger, S., Selarka, D., & Turner, G. (2013, May) *Novel paradigm for investigating the dissociability of executive functions*. Poster presented at the Canadian Neuroscience Meeting, Toronto, ON.
- McIntosh, A. R., Chau, W. K., & Protzner, A. B. (2004). Spatiotemporal analysis of event-related fMRI data using partial least squares. *Neuroimage*, *23*(2), 764-775.
doi:10.1016/j.neuroimage.2004.05.018
- McNab, F., Leroux, G., Strand, F., Thorell, L., Bergman, S., & Klingberg, T. (2008). Common and unique components of inhibition and working memory: An fMRI, within-subjects investigation. *Neuropsychologia*, *46*(11), 2668-2682.
doi:10.1016/j.neuropsychologia.2008.04.023
- Menon, V., & Uddin, L. Q. (2010). Saliency, switching, attention and control: A network model of insula function. *Brain Structure and Function*, *214*(5-6), 655-667.
doi:10.1007/s00429-010-0262-0
- Miyake, A., Friedman, N. P., Emerson, M. J., Witzki, A. H., Howerter, A., & Wager, T. D. (2000). The unity and diversity of executive functions and their contributions to complex "frontal lobe" tasks: A latent variable analysis. *Cognitive Psychology*, *41*(1), 49-100. doi:10.1006/cogp.1999.0734
- Mostofsky, S., & Simmonds, D. (2008). Response inhibition and response selection: two sides of the same coin. *Journal of Cognitive Neuroscience*, *20*(5), 751-761.
doi:10.1162/jocn.2008.20500
- Monsell, S. (2003). Task switching. *Trends in Cognitive Sciences*, *7*(3), 134-140.
doi:10.1016/S1364-6613(03)00028-7

- Niendam, T. A., Laird, A. R., Ray, K. L., Dean, Y. M., Glahn, D. C., & Carter, C. S. (2012). Meta-analytic evidence for a superordinate cognitive control network subserving diverse executive functions. *Cognitive, Affective, & Behavioral Neuroscience, 12*(2), 241-268. doi:10.3758/s13415-011-0083-5
- Owen, A. M., McMillan, K. M., Laird, A. R., & Bullmore, E. (2005). N-back working memory paradigm: A meta-analysis of normative functional neuroimaging studies. *Human Brain Mapping, 25*(1), 46-59. doi: 10.1002/hbm.20131
- Petrides, M., Alivisatos, B., Meyer, E., & Evans, A. C. (1993). Functional activation of the human frontal cortex during the performance of verbal working memory tasks. *Proceedings of the National Academy of Sciences, 90*(3), 878-882. doi:0.1073/pnas.90.3.878
- Ravizza, S. M., & Carter, C. S. (2008). Shifting set about task switching: Behavioral and neural evidence for distinct forms of cognitive flexibility. *Neuropsychologia, 46*(12), 2924-2935. doi:10.1016/j.neuropsychologia.2008.06.006
- Rubia, K., Smith, A. B., Brammer, M. J., & Taylor, E. (2003). Right inferior prefrontal cortex mediates response inhibition while mesial prefrontal cortex is responsible for error detection. *Neuroimage, 20*(1), 351-358. doi:10.1016/S1053-8119(03)00275-1
- Ruge, H., Jamadar, S., Zimmermann, U., & Karayanidis, F. (2013). The many faces of preparatory control in task switching: reviewing a decade of fMRI research. *Human brain mapping, 34*(1), 12-35. doi:10.1002/hbm.21420
- Simmonds, D. J., Pekar, J. J., & Mostofsky, S. H. (2008). Meta-analysis of Go/No-go tasks demonstrating that fMRI activation associated with response inhibition is

- task-dependent. *Neuropsychologia*, 46(1), 224-232. doi:
10.1016/j.neuropsychologia.2007.07.015
- Sohn, M. H., Ursu, S., Anderson, J. R., Stenger, V. A., & Carter, C. S. (2000). The role of prefrontal cortex and posterior parietal cortex in task switching. *Proceedings of the National Academy of Sciences*, 97(24), 13448-13453.
doi:10.1073/pnas.240460497
- Spreng, R. N., Sepulcre, J., Turner, G. R., Stevens, W. D., & Schacter, D. L. (2013). Intrinsic architecture underlying the relations among the default, dorsal attention, and frontoparietal control networks of the human brain. *Journal of Cognitive Neuroscience*, 25(1), 74-86. doi:10.1162/jocn_a_00281
- Stuss, D. T., & Alexander, M. P. (2000). Executive functions and the frontal lobes: a conceptual view. *Psychological research*, 63(3-4), 289-298.
doi:10.1007/s004269900007
- Swanson, R., Cunnington, R., Jackson, G. M., Rorden, C., Peters, A. M., Morris, P. G., & Jackson, S. R. (2003). Cognitive control mechanisms revealed by ERP and fMRI: Evidence from repeated task-switching. *Journal of Cognitive Neuroscience*, 15(6), 785-799. doi:10.1162/089892903322370717
- Sylvester, C. Y. C., Wager, T. D., Lacey, S. C., Hernandez, L., Nichols, T. E., Smith, E. E., & Jonides, J. (2003). Switching attention and resolving interference: fMRI measures of executive functions. *Neuropsychologia*, 41(3), 357-370.
doi:10.1016/S0028-3932(02)00167-7

- Turner, G. R., & Spreng, R. N. (2012). Executive functions and neurocognitive aging: dissociable patterns of brain activity. *Neurobiology of Aging*, 33(4), 826.e1–826.e13. doi:10.1016/j.neurobiolaging.2011.06.005
- Vincent, J. L., Kahn, I., Snyder, A. Z., Raichle, M. E., & Buckner, R. L. (2008). Evidence for a frontoparietal control system revealed by intrinsic functional connectivity. *Journal of Neurophysiology*, 100(6), 3328-3342. doi:10.1152/jn.90355.2008
- Wager, T. D., Jonides, J., & Reading, S. (2004). Neuroimaging studies of shifting attention: A meta-analysis. *Neuroimage*, 22(4), 1679-1693. doi:10.1016/j.neuroimage.2004.03.052
- Wager, T. D., & Smith, E. E. (2003). Neuroimaging studies of working memory: A meta-analysis. *Cognitive, Affective, & Behavioral Neuroscience*, 3(4), 255-274. doi:10.3758/CABN.3.4.255
- Zanto, T. P., & Gazzaley, A. (2009). Neural suppression of irrelevant information underlies optimal working memory performance. *The Journal of Neuroscience*, 29(10), 3059-3066. doi:10.1523/JNEUROSCI.4621-08.2009
- Zelazo, P. D., Carter, A., Reznick, J. S., & Frye, D. (1997). Early development of executive function: A problem-solving framework. *Review of General Psychology*, 1(2), 198. doi:10.1037/1089-2680.1.2.198

Appendices

Table1
Number of Trials per Condition

Condition	Type of Trial (Correct Response)			Total
	Yes	No	Withhold	
Control	<i>66</i>	<i>66</i>	0	132
Updating	<i>66</i>	<i>66</i>	0	132
Inhibition	<i>44</i>	<i>44</i>	<i>44</i>	132
Updating & Inhibition	<i>44</i>	<i>44</i>	<i>44</i>	132
Task Switching	<i>20</i>	<i>20</i>	8	48

Note. Numbers presented in italics are approximations of the number of trials of each type. Since the order of the trials within a block was randomized and the first trial of every block was a task switch trial, exact numbers of each type of trial (yes, no, & withhold) fluctuated by up to 12 trials for each participant. However, the total number of trials for each condition was constant across all participants.

Table 2
Mean Accuracy and Reaction Times

Condition	% Accuracy	Mean RT
Control	96.34 (0.03)	765.17 (139.71)
Updating	82.73 (0.15)	694.70 (185.16)
Inhibition	91.47 (0.05)	873.20 (150.51)
Inhibit trials	75.80 (0.14)	n/a (n/a)
Updating & Inhibition	70.25 (0.12)	939.40 (208.38)
Task Switch	89.96 (0.10)	947.40 (182.22)
Overall	85.96 (0.07)	810.04 (144.49)

Note. Mean (SD) of % accuracy and mean reaction time (in ms) for correct trials on each condition in the study for all participants included in the analysis. The inhibition condition includes performance during the “double yellow” blocks, as well as specific inhibit trials, where the correct response was to withhold.

Table 3
Paired t-tests for % Accuracy

Pairwise Comparison	Mean 1	Mean 2	<i>t</i>	<i>df</i>	<i>p value</i> ($\alpha=.005$)
Control – Updating	96.34	82.73	4.43	21	.000*
Control – Inhibition	96.34	91.47	6.50	21	.000*
Control – Updating & Inhibition	96.34	70.25	11.14	21	.000*
Control – Task Switch	96.34	89.96	3.46	21	.002*
Updating – Inhibition	82.73	91.47	-2.97	21	.007
Updating – Updating & Inhibition	82.73	70.25	6.89	21	.000*
Updating – Task Switch	82.73	89.96	-2.11	21	.047
Inhibition – Updating & Inhibition	91.47	70.25	9.69	21	.000*
Inhibition – Task Switch	91.47	89.96	.82	21	.424
Updating & Inhibition – Task Switch	70.25	89.96	-7.16	21	.000*

Note. Pairwise *t*-tests comparison of % accuracy on each condition for all participants included in the analysis. * denotes statistically significant differences between means, after a Bonferroni correction for multiple comparisons has been applied.

Table 4
Paired t-tests for mean RT

Pairwise Comparison	Mean 1	Mean 2	<i>t</i>	<i>df</i>	<i>p value</i> ($\alpha=.005$)
Control – Updating	765.17	694.70	2.40	21	.026
Control – Inhibition	765.17	873.20	-9.34	21	.000*
Control – Updating & Inhibition	765.17	939.40	-4.74	21	.000*
Control – Task Switch	765.17	947.40	-9.19	21	.000*
Updating – Inhibition	694.70	873.20	-5.25	21	.000*
Updating – Updating & Inhibition	694.70	939.40	-7.74	21	.000*
Updating – Task Switch	694.70	947.40	-7.21	21	.000*
Inhibition – Updating & Inhibition	873.20	939.40	-1.73	21	.098
Inhibition – Task Switch	873.20	947.40	-3.47	21	.002*
Updating & Inhibition – Task Switch	939.40	947.40	-.21	21	.837

Note. Pairwise *t*-tests comparison of mean RT (in ms) for correct trials on each condition for all participants included in the analysis. * denotes statistically significant differences between means, after a Bonferroni correction for multiple comparisons has been applied.

Table 5
 Cluster reports for LV1 & LV2 of the Full-Model PLS Analysis

Cluster Location	Cluster Size (in voxels)	MNI Coordinates			Brodmann Area	BSR
		x	y	z		
LV1 (BSR 5.0)						
Left superior parietal lobule	628	-36	-72	45	8	10.73
Left precuneus	238	-3	-69	42	7	10.52
Left posterior cingulate gyrus	220	0	-30	36	31	10.70
Right superior frontal gyrus	199	3	6	54	6	9.10
Right cuneus	31	9	-87	6	17	8.41
Right precuneus	24	36	-72	42	19	6.42
Left middle frontal gyrus	20	-24	0	63	6	6.67
LV2 (BSR 2.5)						
Right middle frontal gyrus	45	42	42	-6	47	4.56
Left inferior frontal gyrus	65	-39	24	-9	47	4.32
Left superior frontal gyrus	22	-6	42	51	8	4.23
Right inferior frontal gyrus	22	51	21	12	45	4.23
Right fusiform gyrus	16	45	-3	-24	20	4.16
Left superior frontal gyrus	15	-15	42	36	9	3.38

Note. Only Positive clusters are reported, for full cluster reports, see supplementary tables. BSR = Bootstrap ratio. BSR for LV1 was set at 5.0 ($p < .001$) to create a more conservative and concise cluster report. For LV2, the original Bootstrap ratio of 2.5 ($p < .0124$) was used. Minimum cluster size 15 voxels. MNI Coordinates and BSR value are reported for cluster maxima.

Table 6
Cluster reports for the Control & Updating Analysis

Cluster Location	Cluster Size (in voxels)	MNI Coordinates			Brodmann Area	BSR
		x	y	z		
LV1 (BSR 3.0)						
Right middle frontal gyrus	315	42	28	15	10	5.95
Right inferior frontal gyrus	278	48	9	27	9	6.19
Medial superior frontal gyrus	250	0	30	48	8	6.11
Right inferior parietal lobule	238	51	-39	42	40	5.71
Right superior frontal gyrus	110	30	12	57	6	5.08
Left inferior frontal gyrus	72	-36	18	-3	47	5.18
Right superior parietal lobule	56	21	-63	63	7	5.50
Left middle frontal gyrus	36	-42	30	27	46	4.03
Left inferior parietal lobule	36	-57	-33	42	40	4.58
Left superior frontal gyrus	32	-24	3	57	6	4.59
Right precuneus	23	30	-72	39	19	4.72
Right caudate	21	15	15	9	--	4.82
Left inferior parietal lobule	20	-36	-39	39	40	4.72

Note. Only Positive (updating-related) clusters are reported, for full cluster reports, see supplementary tables. BSR = Bootstrap ratio. BSR for LV1 was set at 3.0 ($p < .003$) to create a more conservative and concise cluster report. Minimum cluster size 15 voxels. MNI Coordinates and BSR value are reported for cluster maxima.

Table 7
Cluster reports for the Control & Inhibition Analysis

Cluster Location	Cluster Size (in voxels)	MNI Coordinates			Brodmann Area	BSR
		x	y	z		
LV1 (BSR 2.5)						
Right inferior frontal gyrus	37	51	21	12	45	5.62
Left middle frontal gyrus	100	-36	51	-3	10	4.79
Right inferior frontal gyrus	15	42	24	0	47	4.25
Right middle frontal gyrus	85	42	45	-3	10	4.24
Left medial frontal gyrus	10	-9	39	39	8	3.94
Right superior frontal gyrus	27	21	27	57	6	3.87

Note. Only Positive (inhibition-related) clusters are reported, for full cluster reports, see supplementary tables. BSR = Bootstrap ratio. The original Bootstrap ratio of 2.5 ($p < .0124$) was used. Minimum cluster size 10 voxels. MNI Coordinates and BSR value are reported for cluster maxima.

Table 8
Cluster reports for the Control & Task Switching Analysis

Cluster Location	Cluster Size (in voxels)	MNI Coordinates			Brodmann Area	BSR
		x	y	z		
LV1 (BSR 5.0)						
Left superior parietal lobule	444	-36	-72	45	7	10.73
Left precuneus	198	-3	-72	42	7	10.21
Left posterior parietal	177	0	-33	36	31	9.23
Right angular gyrus	95	48	-63	33	39	8.19
Right superior medial frontal gyrus	87	3	9	54	6	9.21
Left middle frontal gyrus	32	-42	33	30	9	6.23
Left precentral gyrus	24	-36	-21	57	4	7.32
Left middle frontal gyrus	21	-24	-3	60	6	5.90
Left cingulate gyrus	20	0	9	39	24	6.02

Note. Only Positive (task-switching-related) clusters are reported, for full cluster reports, see supplementary tables. BSR = Bootstrap ratio. BSR for LV1 was set at 5.0 ($p < .001$) to create a more conservative and concise cluster report. Minimum cluster size 15 voxels. MNI Coordinates and BSR value are reported for cluster maxima.

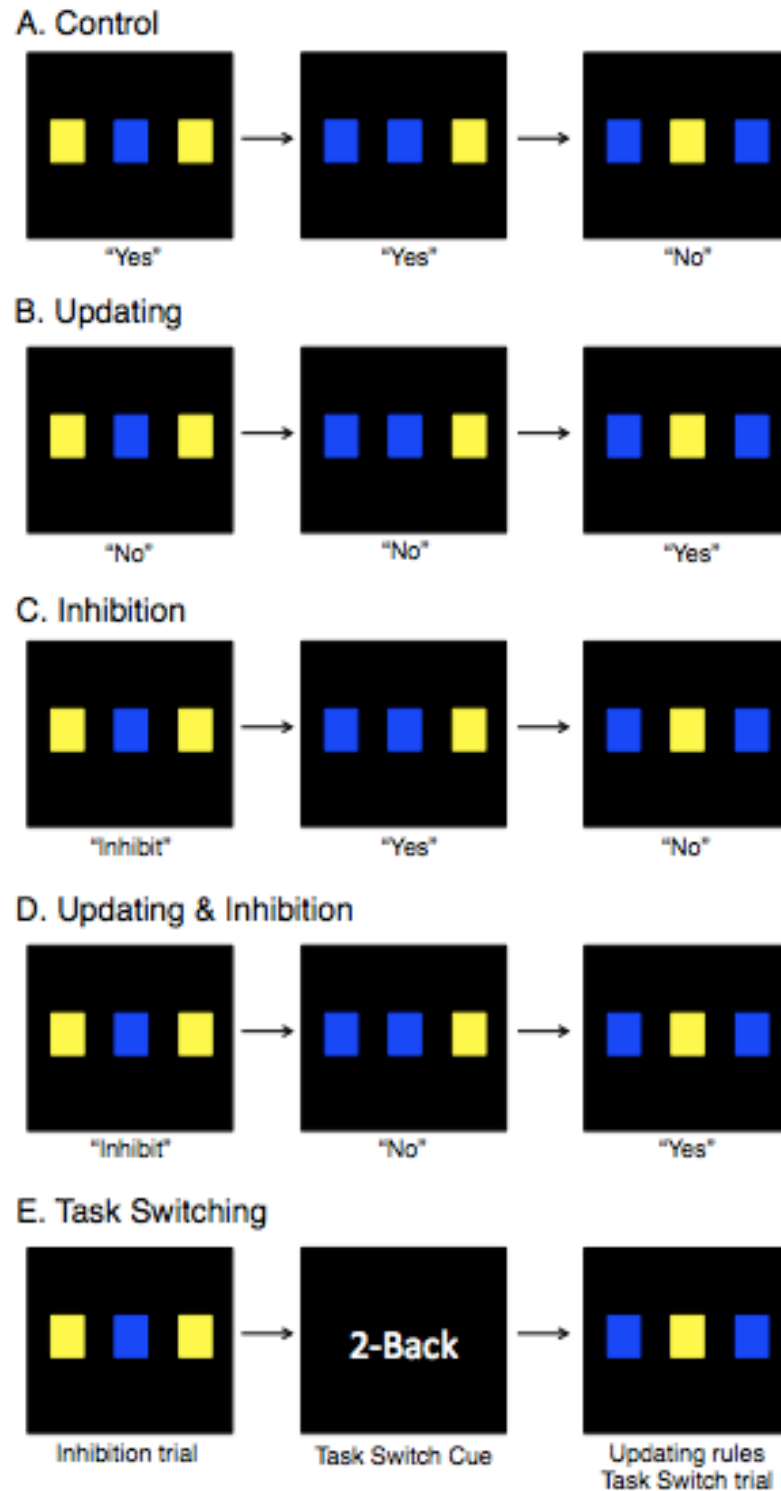


Figure 1. Overview of the different tasks used in the study. Panel A. The “Middle-Blue” task (Baseline Control): “Is the middle-square blue?” Panel B. “2-Back” task (Updating): “Was the middle-square blue two trials ago?” Panel C. “Double-Yellow” task (Inhibition): “Is the middle square blue? If any and only two squares are yellow, then do not answer.” Panel D. “Double-Yellow 2-Back” task (Inhibition & Updating): “Was the middle-square blue two trials ago? If any and only two squares are currently yellow, do not answer.” Panel E. Switching was embedded within blocks; participants were given a cue to notify them which task is next. Responses underneath the images represent correct responses.

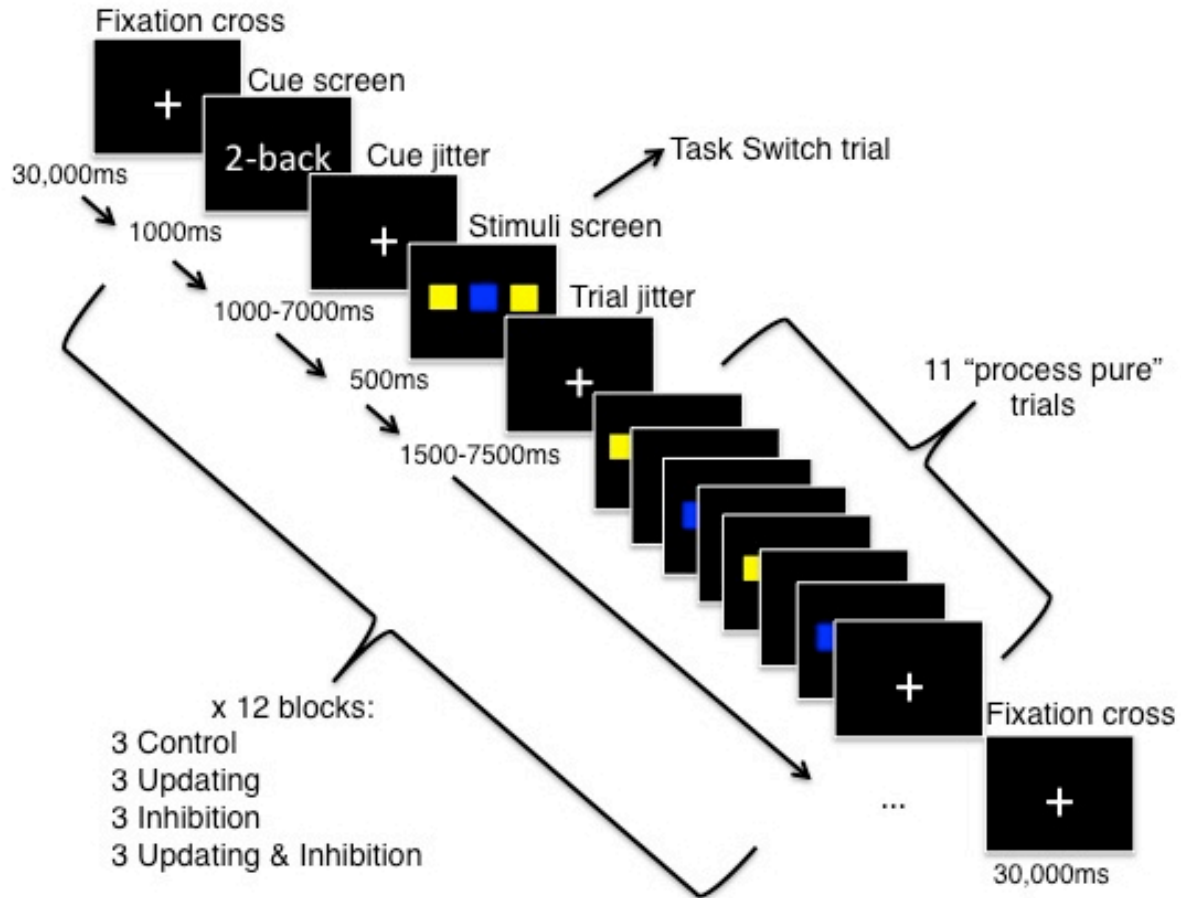


Figure 2. Overview of the structure of a run. There were 12 trials/block: 1 task switch trial and 11 or condition-specific or “process pure” trials. There were 12 blocks/run and 4 runs/session (3 blocks of each condition in a given run, and 12 blocks of each condition overall). A fixation cross was presented at the beginning and end of each run for 30s.

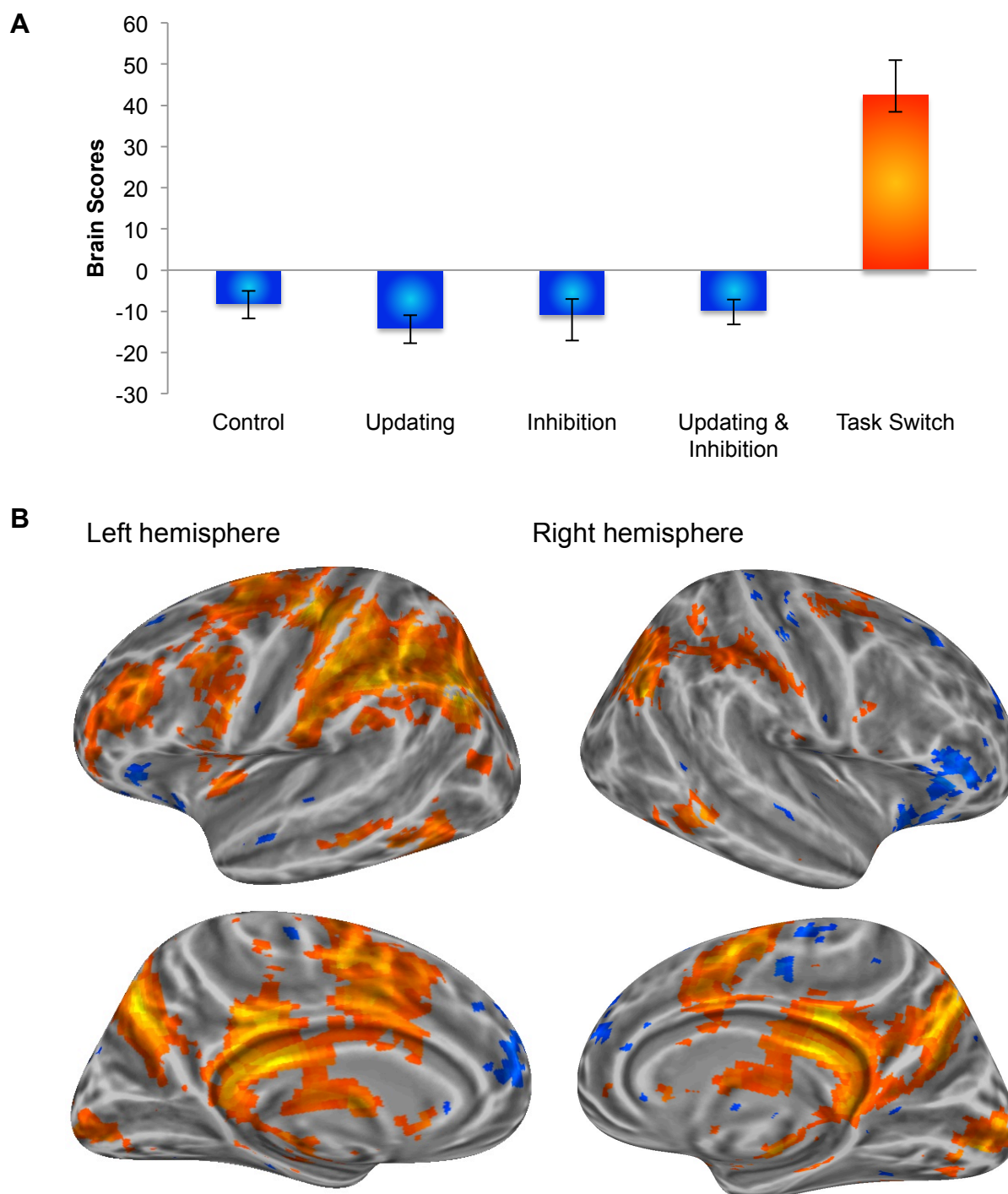


Figure 3. Panel A. PLS Brain Scores for LV1 of the full-model analysis (all condition types included). Error bars represent 95% confidence intervals determined by bootstrapping analysis. Panel B. The brain pattern identified by this LV depicted on cortical surface maps (top row: lateral surface, bottom row: medial surface). Warmer colours represent activity related to the task switch condition; cool colours represent the other conditions. Images were generated using a BSR threshold of ± 2.5 ($p < .0124$) and minimum cluster size of 5 voxels.

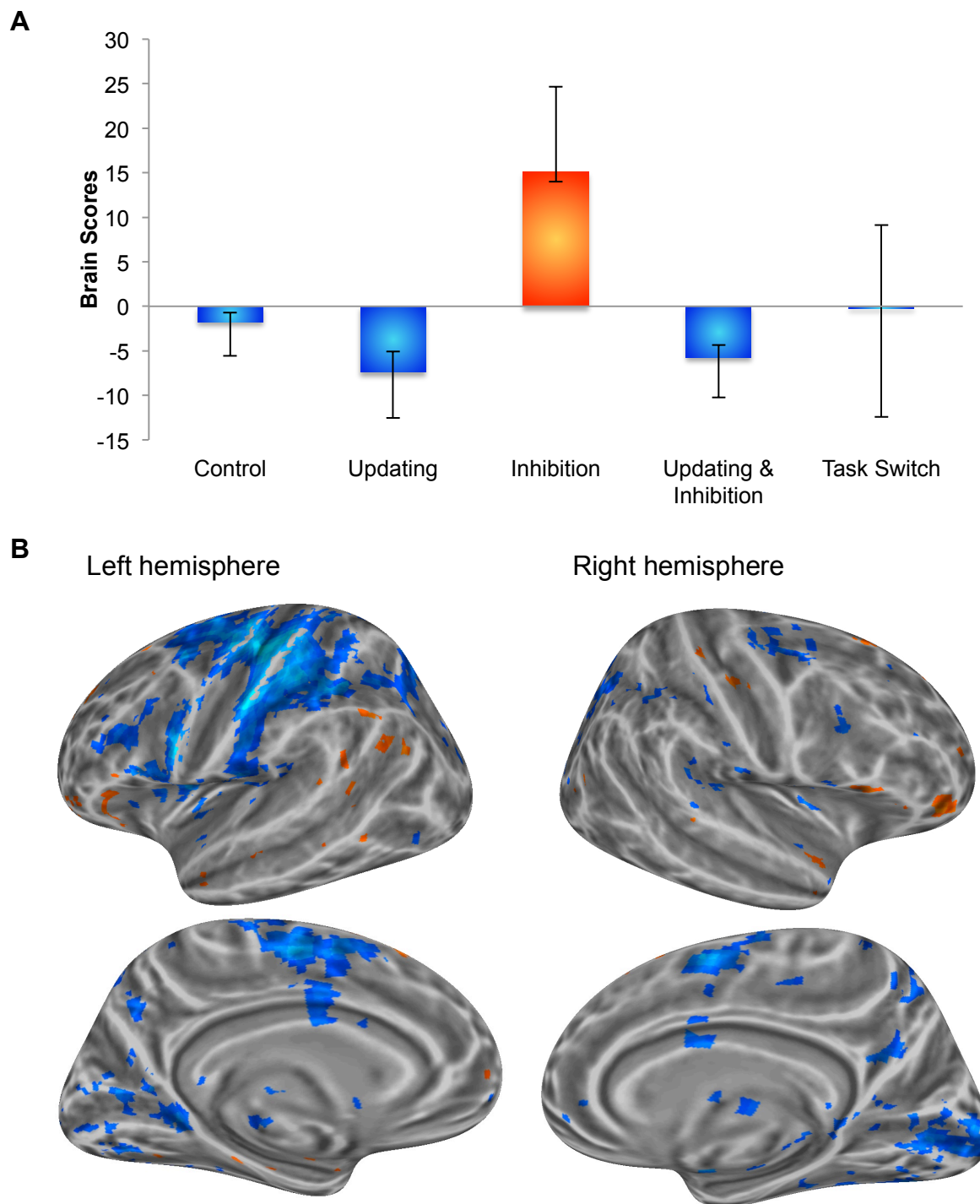


Figure 4. Panel A. PLS Brain Scores for LV2 of the full-model analysis (all condition types included). Error bars represent 95% confidence intervals determined by bootstrapping analysis. Panel B. The brain pattern identified by this LV depicted on cortical surface maps (top row: lateral surface, bottom row: medial surface). Warmer colours represent activity associated with Inhibition events; cool colours represent the other conditions. Images were generated using a BSR threshold of ± 2.5 ($p < .0124$) and minimum cluster size of 5 voxels.

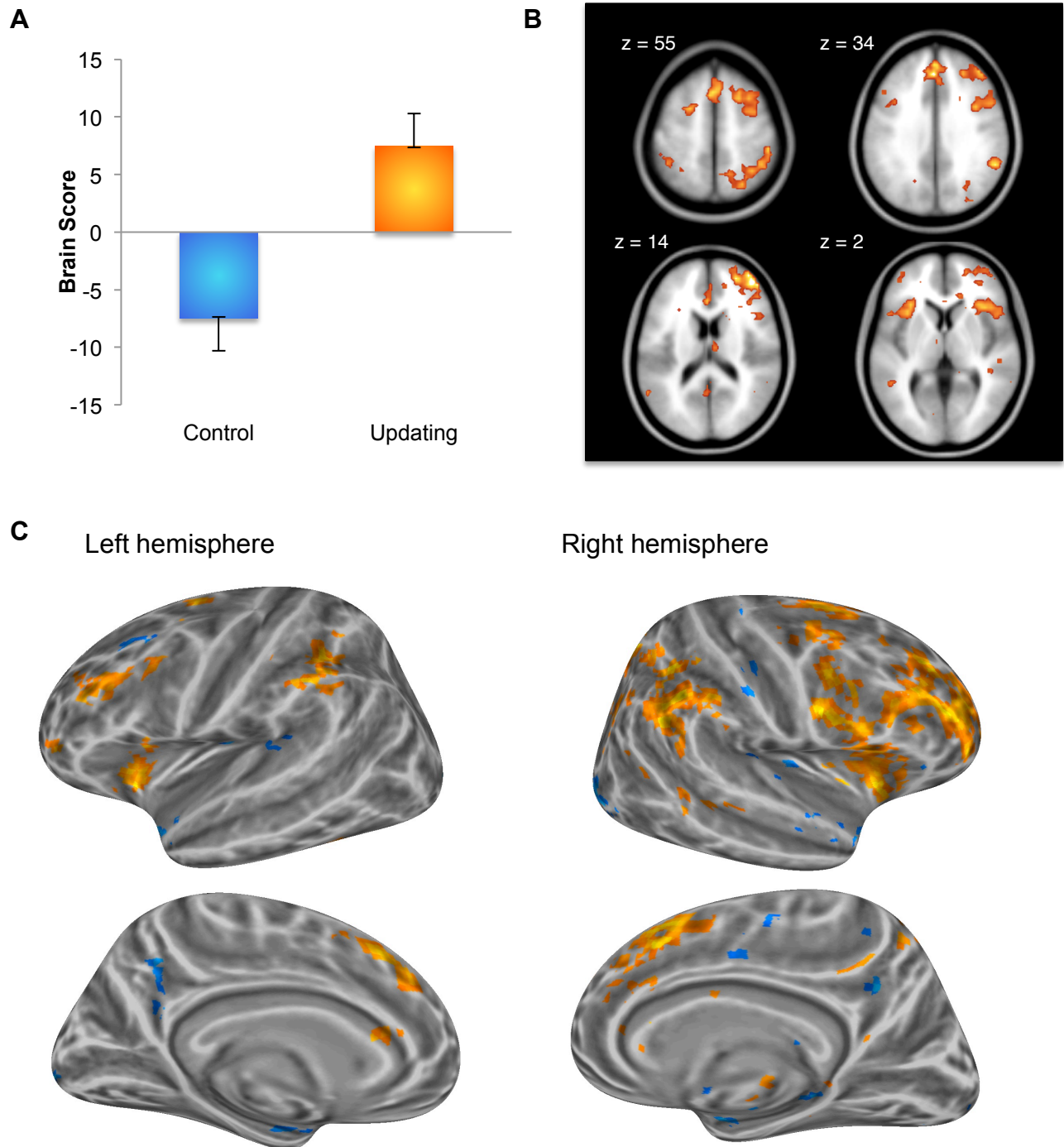


Figure 5. Panel A. PLS Brain Scores for LV1 in the control & updating analysis. Error bars represent 95% confidence intervals determined by bootstrapping analysis. Panel B. 4 axial slices of the updating-related pattern of activation depicting right superior parietal ($z = 55$), superior medial frontal ($z = 55$, $z = 34$), bilateral insular ($z = 2$) and left lateral PFC (all 4 slices) activation. The coordinates are reported in MNI space. Panel C. The overall brain pattern of activity identified in this analysis depicted on cortical surface maps (top row: lateral surface, bottom row: medial surface). Warmer colours represent activity related to the updating condition; cool colours represent the control condition. Images were generated using a BSR threshold of ± 2.5 ($p < .0124$) and minimum cluster size of 5 voxels.

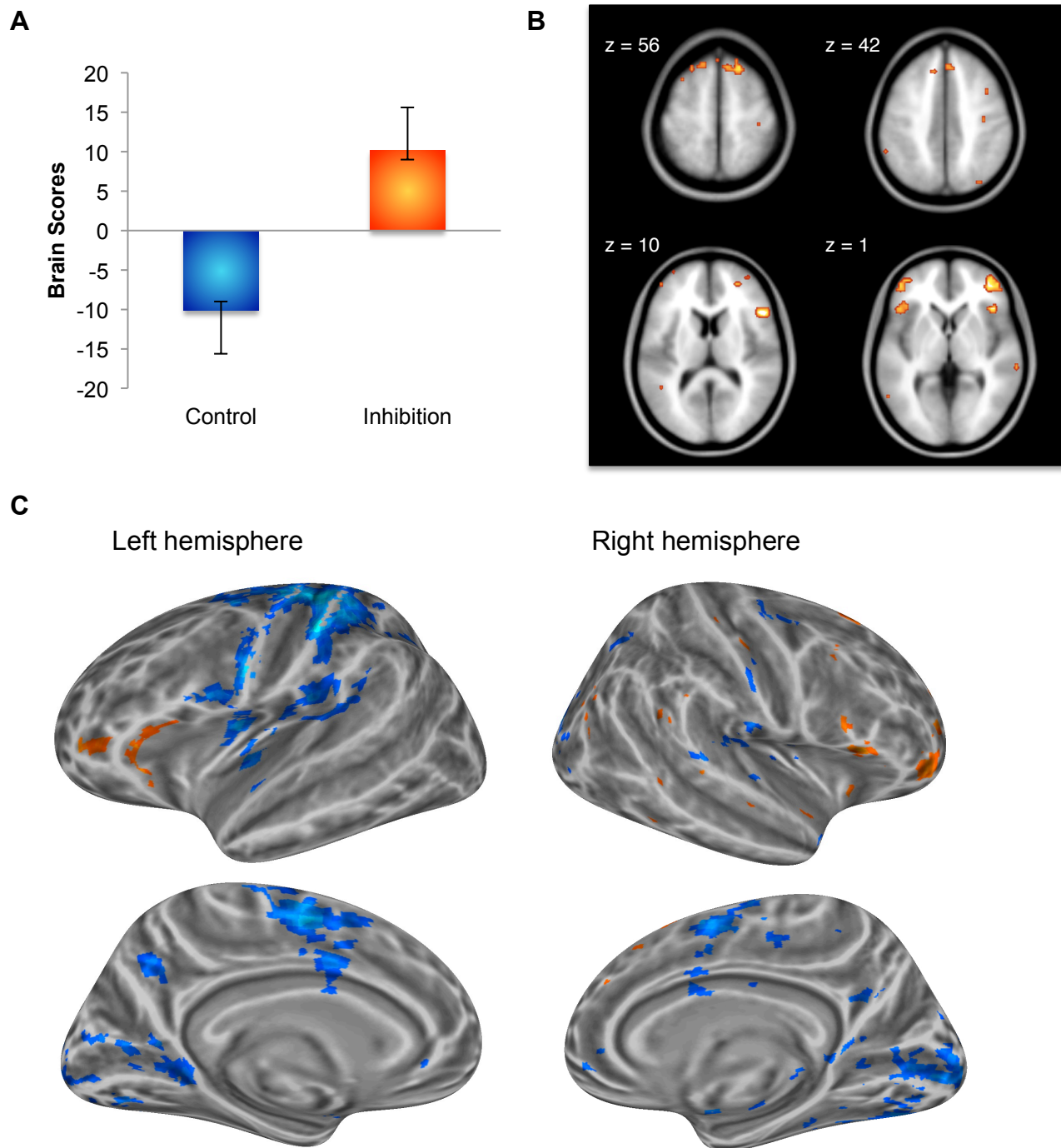


Figure 6. Panel A. PLS Brain Scores for LV1 in the control & inhibition trials analysis. Error bars represent 95% confidence intervals determined by bootstrapping analysis. Panel B. 4 axial slices of the inhibition-related pattern of activation depicting superior frontal ($z = 56$), pre-SMA ($z = 42$), right inferior frontal ($z = 10$) and bilateral anterior inferior and middle frontal gyrus ($z=1$) activation. The coordinates are reported in MNI space. Panel C. The overall pattern of brain activity identified in this analysis depicted on cortical surface maps (top row: lateral surface, bottom row: medial surface). Warmer colours represent activity related to inhibition trials; cool colours represent the control condition (including the left motor cortex). Images were generated using a BSR threshold of ± 2.5 ($p < .0124$) and minimum cluster size of 5 voxels.

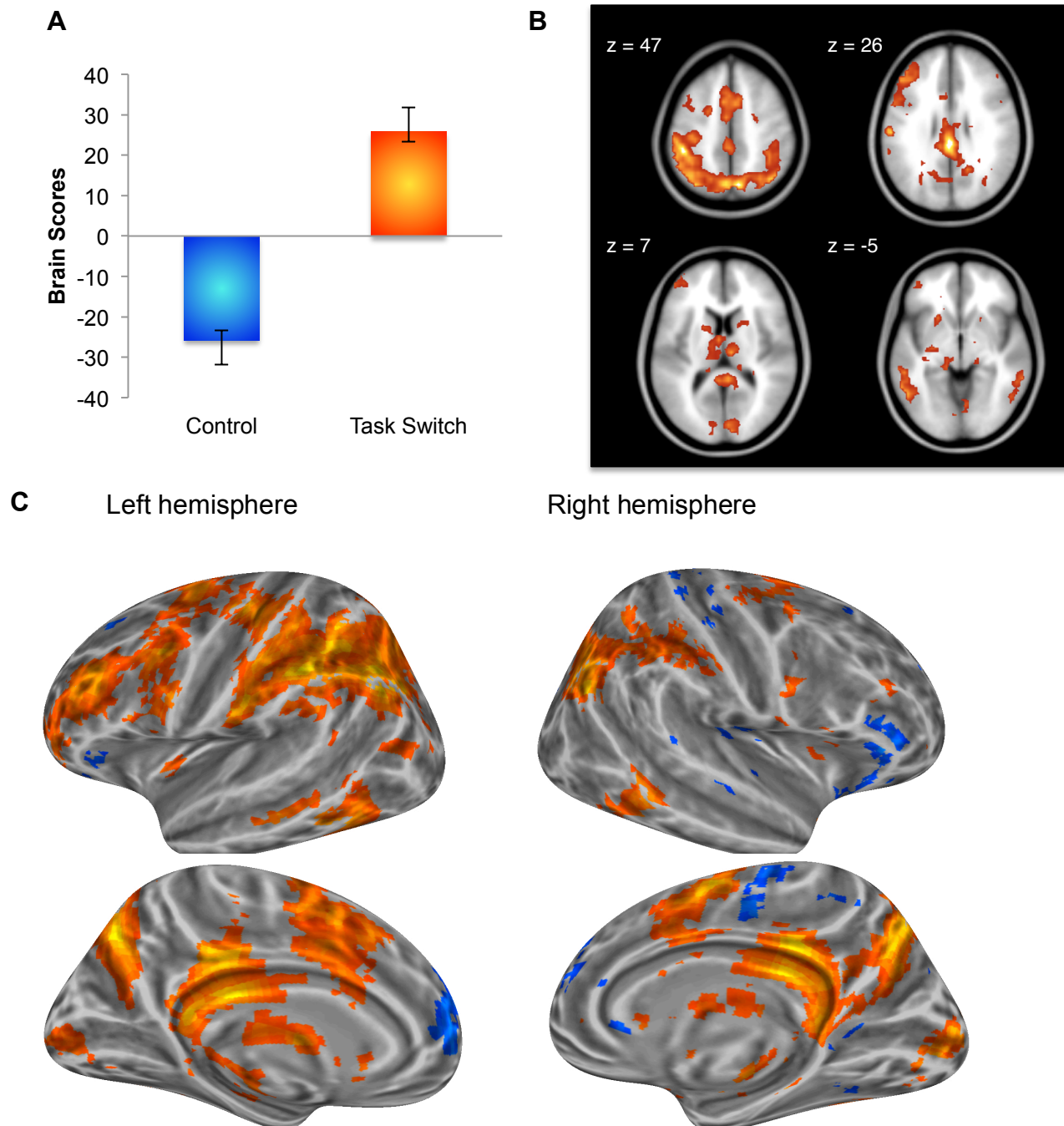


Figure 7. Panel A. PLS Brain Scores for LV1 in the control & task switching analysis. Error bars represent 95% confidence intervals determined by bootstrapping analysis. Panel B. 4 axial slices of the task-switching-related pattern of activation depicting wide-spread, mostly left-lateralized activity, including the bilateral superior parietal lobules, precuneus and superior medial PFC ($z = 47$), posterior cingulate and left anterior middle frontal gyrus, bilateral thalamus ($z = 26$, $z = 7$), cuneus ($z = 7$), and bilateral inferior/middle temporal gyrus ($z = -5$). The coordinates are reported in MNI space. Panel C. The overall pattern of brain activation identified in this analysis depicted on cortical surface maps (top row: lateral surface, bottom row: medial surface). Warmer colours represent activity related to task switch trials; cool colours represent the control condition. Images were generated using a BSR threshold of ± 2.5 ($p < .0124$) and minimum cluster size of 5 voxels.

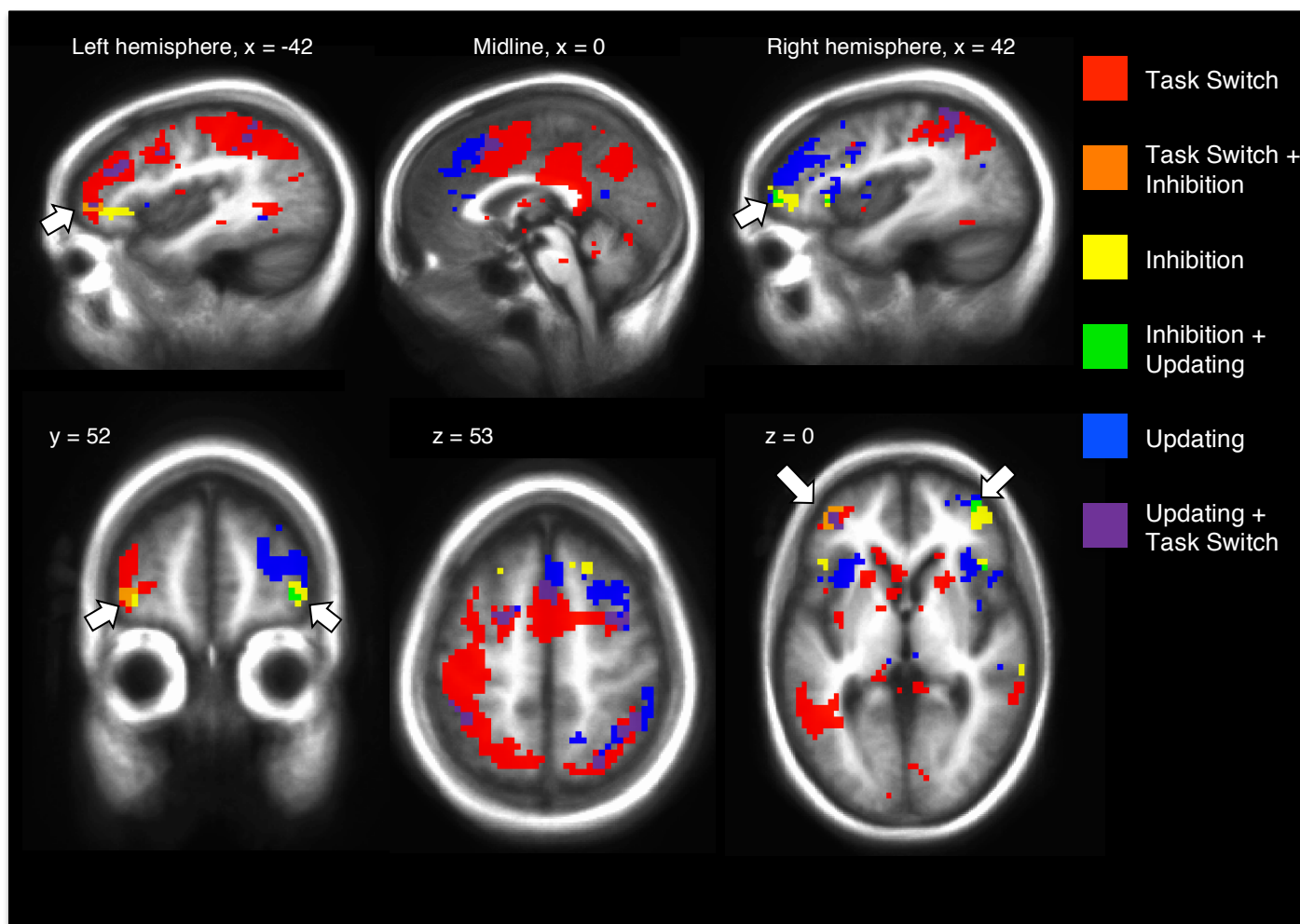


Figure 8. Conjunction analysis results. The three executive processes were assigned primary colours (task switch: red, updating: blue, inhibition: yellow) and regions of overlap between them were colour-coded correspondingly (see colour legend). Areas of overlap between inhibition and the two other executive control processes are pointed out with the use of arrows. Though there was no point of complete overlap, all three executive processes showed activation in the left anterior middle frontal gyrus (best seen in $z = 0$). Images were generated using the three individual PLS analyses in which the control condition was directly analyzed with each executive process of interest (BSR threshold of ± 2.5 , $p < .0124$, no minimum cluster size). Images are presented in radiological convention, slice values are reported in MNI space.

Supplementary Materials

Supplementary Table 1
Paired Wilcoxon Signed Rank tests for % Accuracy

Pairwise Comparison	Mean Rank 1	Mean Rank 2	Z	<i>p</i> value ($\alpha=.005$)
Control – Updating	4.73	2.61	3.74	.000*
Control – Inhibition	4.73	3.41	4.01	.000*
Control – Updating & Inhibition	4.73	1.14	4.11	.000*
Control – Task Switch	4.73	3.11	3.49	.000*
Updating – Inhibition	2.61	3.41	2.84	.005
Updating – Updating & Inhibition	2.61	1.14	3.69	.000*
Updating – Task Switch	2.61	3.11	2.19	.028
Inhibition – Updating & Inhibition	3.41	1.14	4.11	.000*
Inhibition – Task Switch	3.41	3.11	.50	.615
Updating & Inhibition – Task Switch	1.14	3.11	3.95	.000*

Note. Follow-up pairwise *Wilcoxon* tests for the non-parametric Friedman analysis of the % accuracy data. *Wilcoxon* tests are comparing the mean rank of % accuracy for each condition (higher mean rank is associated with better performance in that condition). * denotes statistically significant differences between mean ranks, after a Bonferroni correction for multiple comparisons has been applied.

Supplementary Table 2
Paired t-tests for median RT

Pairwise Comparison	Mean 1	Mean 2	<i>t</i>	<i>df</i>	<i>p value</i> ($\alpha=.005$)
Control – Updating	720.00	621.52	3.46	21	.002*
Control – Inhibition	720.00	833.77	-9.14	21	.000*
Control – Updating & Inhibition	720.00	876.00	-4.12	21	.000*
Control – Task Switch	720.00	909.82	-8.51	21	.000*
Updating – Inhibition	621.52	833.77	-6.40	21	.000*
Updating – Updating & Inhibition	621.52	876.00	-7.22	21	.000*
Updating – Task Switch	621.52	909.82	-9.14	21	.000*
Inhibition – Updating & Inhibition	833.77	876.00	-1.06	21	.302
Inhibition – Task Switch	833.77	909.82	-3.32	21	.003*
Updating & Inhibition – Task Switch	876.00	909.82	-.96	21	.350

Note. Pairwise *t*-tests comparisons of median RT (in ms) for correct trials on each condition for all participants included in the analysis. * denotes statistically significant differences between means, after a Bonferroni correction for multiple comparisons has been applied.

Supplementary Table 3
 Full Cluster report for LV1 from the Full-Model PLS Analysis

Cluster peak location	Hemisphere	MNI coordinates			BA	BSR	Cluster Size (in voxels)
		X	Y	Z			
Task Switching							
Superior Parietal Lobule	Left	-36	-72	45	7	10.73	8184
Cuneus	Right	9	-87	6	17	8.41	1038
Parahippocampal Gyrus	Right	21	-24	-12	35	7.09	60
Middle Frontal Gyrus	Left	-42	42	18	10	5.91	336
Middle Temporal Gyrus	Right	66	-42	-3	21	5.39	60
Parahippocampal Gyrus	Right	33	-12	-12	--	4.47	17
Superior Temporal Gyrus	Right	39	9	-27	38	4.10	13
Middle Occipital Gyrus	Right	54	-63	-9	37	4.09	19
Precentral Gyrus	Right	45	6	33	9	3.82	14
Substantia Nigra	Left	-6	-15	-12	--	3.65	10
Insula	Left	-33	12	9	13	3.47	11
Insula	Right	30	-33	24	13	3.42	13
All Other Conditions							
Inferior Frontal Gyrus	Right	48	30	3	45	-5.90	151
Inferior Frontal Gyrus	Right	39	27	-12	47	-4.78	72
Medial Frontal Gyrus	Right	12	-12	48	6	-4.70	15
Medial Frontal Gyrus	Left	-3	51	12	10	-4.44	189
Inferior Frontal Gyrus	Left	-39	33	-3	47	-4.29	36
Inferior Frontal Gyrus	Left	-30	18	-12	47	-4.00	21
Superior Frontal Gyrus	Right	18	24	45	8	-3.88	20
Medial Frontal Gyrus	Right	6	-18	63	6	-3.85	13
Precentral Gyrus	Right	39	-18	48	4	-3.70	18
Middle Frontal Gyrus	Left	-21	30	42	8	-3.61	10
Superior Frontal Gyrus	Right	24	54	27	9	-3.40	19
Precentral Gyrus	Right	30	-27	63	4	-3.18	18
Precentral Gyrus	Right	18	-30	66	4	-3.14	10

Note. BA = Brodmann Area, BSR = Bootstrap ratio. This cluster report was created using a minimum BSR for +/-2.5 ($p < .0124$) and a minimum cluster size 10 voxels. MNI Coordinates and BSR value are reported for cluster maxima.

Supplementary Table 4
 Full Cluster report for LV2 from the Full-Model PLS Analysis

Cluster peak location	Hemisphere	MNI Coordinates			BA	BSR	Cluster Size (in voxels)
		X	Y	Z			
Inhibition							
Middle Frontal Gyrus	Right	42	42	-6	47	4.56	45
Inferior Frontal Gyrus	Left	-39	24	-9	47	4.32	65
Superior Frontal Gyrus	Left	-6	42	51	8	4.23	22
Inferior Frontal Gyrus	Right	51	21	12	45	4.23	22
Fusiform Gyrus	Right	45	-3	-24	20	4.16	16
Middle Temporal Gyrus	Left	-42	-66	30	39	3.86	12
Superior Frontal Gyrus	Left	-15	42	36	9	3.83	15
Inferior Parietal Lobule	Left	-51	-60	42	39	3.80	11
Superior Frontal Gyrus	Right	21	27	57	6	3.56	14
All Other Conditions							
Precentral Gyrus	Left	-30	-9	57	6	-8.76	2241
Inferior Frontal Gyrus	Left	-57	6	27	9	-7.19	308
Thalamus	Left	-15	-27	6	--	-6.67	131
Culmen	Right	24	-51	-18	--	-6.27	353
Putamen	Right	18	6	0	--	-5.72	29
Declive	Left	-18	-75	-12	--	-5.68	91
Middle Frontal Gyrus	Right	30	-6	54	6	-5.53	80
Amygdala	Right	18	-9	-12	--	-5.15	13
Posterior Cingulate	Left	-15	-57	15	30	-4.94	22
Middle Occipital Gyrus	Right	12	-93	15	18	-4.83	211
Lingual Gyrus	Left	-18	-48	0	--	-4.78	57
Anterior Cingulate	Right	9	36	0	24	-4.72	69
Lingual Gyrus	Left	0	-78	-6	18	-4.72	10
Superior Frontal Gyrus	Right	21	45	3	--	-4.42	14
Parahippocampal Gyrus	Right	30	-51	6	30	-4.37	51
Superior Temporal Gyrus	Right	42	-33	18	41	-4.29	23
Clastrum	Left	-33	-15	-3	--	-4.28	39
Middle Frontal Gyrus	Right	30	39	42	8	-4.09	19
Thalamus	Right	6	-15	9	--	-4.04	19
Insula	Right	39	0	9	13	-3.97	13
Thalamus	Right	18	-12	12	--	-3.91	29
Postcentral Gyrus	Right	51	-33	51	40	-3.81	20
Insula	Left	-33	12	12	13	-3.72	18
Posterior Cingulate	Left	-3	-60	6	30	-3.64	10
Sub-Gyral	Right	36	-42	36	40	-3.62	27

Middle Frontal Gyrus	Left	-24	30	39	8	-3.55	12
Middle Frontal Gyrus	Right	33	12	27	9	-3.51	10
Posterior Cingulate	Left	-6	-66	15	31	-3.42	13
Middle Occipital Gyrus	Left	-21	-87	15	18	-3.30	13
Lingual Gyrus	Left	-6	-84	3	17	-3.28	10
Declive	Left	-36	-57	-18	*	-2.98	11

Note. BA = Brodmann Area, BSR = Bootstrap ratio. This cluster report was created using a minimum BSR for +/-2.5 ($p < .0124$) and a minimum cluster size 10 voxels. MNI Coordinates and BSR value are reported for cluster maxima.

Supplementary Table 5
 Full Cluster report for LV1 from the Updating & Control PLS analysis

Cluster peak location	Hemisphere	MNI Coordinates			BA	BSR	Cluster Size (in voxels)
		X	Y	Z			
Updating							
Inferior Frontal Gyrus	Right	48	9	27	9	6.19	1649
Inferior Parietal Lobule	Right	51	-39	42	40	5.71	528
Inferior Frontal Gyrus	Left	-36	18	-3	47	5.18	134
Medial Frontal Gyrus	Right	3	42	18	9	4.90	26
Caudate	Right	15	15	9	--	4.82	31
Precuneus	Right	30	-72	39	19	4.72	74
Inferior Parietal Lobule	Left	-36	-39	39	40	4.71	122
Sub-Gyral	Left	-24	3	57	6	4.59	55
Fusiform Gyrus	Left	-42	-51	-9	37	4.21	15
Inferior Frontal Gyrus	Left	-39	45	0	--	4.14	17
Middle Frontal Gyrus	Left	-42	30	27	9	4.03	80
Precentral Gyrus	Left	-42	6	36	9	4.00	35
Middle Temporal Gyrus	Right	54	-45	9	21	3.42	16
Thalamus	Right	9	-15	15	--	3.39	22
Posterior Cingulate	Left	0	-57	18	23	3.36	10
Control							
Cuneus	Left	-18	-96	3	--	-5.02	29
Culmen	Right	24	-45	-21	--	-4.73	26
Middle Occipital Gyrus	Right	30	-87	9	19	-4.68	62
Sub-Gyral	Right	36	-9	-18	20	-4.49	21
Parahippocampal Gyrus	Left	-24	-21	-9	28	-4.44	12
Sub-Gyral	Left	-45	-18	-18	20	-4.27	32
Thalamus	Left	-12	-30	18	--	-4.24	28
Middle Temporal Gyrus	Left	-39	3	-24	21	-4.21	43
Superior Temporal Gyrus	Right	42	18	-24	38	-4.18	19
Hippocampus	Right	27	-39	0	--	-4.00	12
Precuneus	Left	-12	-48	27	31	-3.98	18
Precuneus	Left	-9	-51	42	7	-3.78	29
Transverse Temporal Gyrus	Left	-33	-36	15	41	-3.71	19
Insula	Left	-36	-18	21	13	-3.67	23
Parahippocampal Gyrus	Left	-36	-45	0	19	-3.49	11
Insula	Right	36	-21	12	13	-3.48	10

Cingulate Gyrus	Left	-3	-39	30	31	-3.48	11
Middle Frontal Gyrus	Left	-30	24	42	8	-3.35	18
Medial Frontal Gyrus	Right	3	-3	51	6	-3.23	13
Cuneus	Left	-18	-78	21	18	-3.22	10

Note. BA = Brodmann Area, BSR = Bootstrap ratio. This cluster report was created using a minimum BSR for +/-2.5 ($p < .0124$) and a minimum cluster size 10 voxels. MNI Coordinates and BSR value are reported for cluster maxima.

Supplementary Table 6

Full Cluster report for LV1 from the Inhibition & Control PLS Analysis

Cluster peak location	Hemisphere	MNI Coordinates			BA	BSR	Cluster Size (in voxels)
		X	Y	Z			
Inhibition							
Inferior Frontal Gyrus	Right	51	21	12	45	5.62	37
Middle Frontal Gyrus	Left	-36	51	-3	10	4.79	100
Inferior Frontal Gyrus	Right	42	24	0	47	4.25	15
Middle Frontal Gyrus	Right	42	45	-3	10	4.24	85
Medial Frontal Gyrus	Left	-9	39	39	8	3.94	10
Superior Frontal Gyrus	Right	21	27	57	6	3.87	27
Control							
Postcentral Gyrus	Left	-57	-18	45	2	-8.51	1817
Culmen	Right	24	-51	-21	--	-6.70	581
Thalamus	Left	-15	-27	6	--	-5.57	113
Middle Frontal Gyrus	Right	30	-6	54	6	-5.10	39
Amygdala	Left	-24	-3	-9	--	-4.93	29
Superior Parietal Lobule	Left	-24	-54	42	7	-4.86	102
Declive	Left	-18	-75	-12	--	-4.78	149
Posterior Cingulate	Left	-12	-54	15	30	-4.63	28
Amygdala	Right	18	-9	-9	--	-4.59	11
Clastrum	Left	-33	-18	9	--	-4.47	40
Parahippocampal Gyrus	Right	27	-51	6	30	-4.29	35
Clastrum	Right	21	27	6	--	-4.19	19
Putamen	Left	-24	6	9	--	-4.07	12
Lingual Gyrus	Left	-21	-48	0	--	-4.03	60
Postcentral Gyrus	Right	63	-18	18	40	-3.85	26
Lingual Gyrus	Left	0	-78	-6	18	-3.80	10
Posterior Cingulate	Right	18	-54	15	30	-3.78	12
Superior Temporal Gyrus	Right	42	-30	15	41	-3.74	28
Thalamus	Left	-27	-30	9	--	-3.66	13
Sub-Gyral	Right	36	-45	33	40	-3.55	27
Middle Frontal Gyrus	Left	-27	27	42	8	-3.52	11

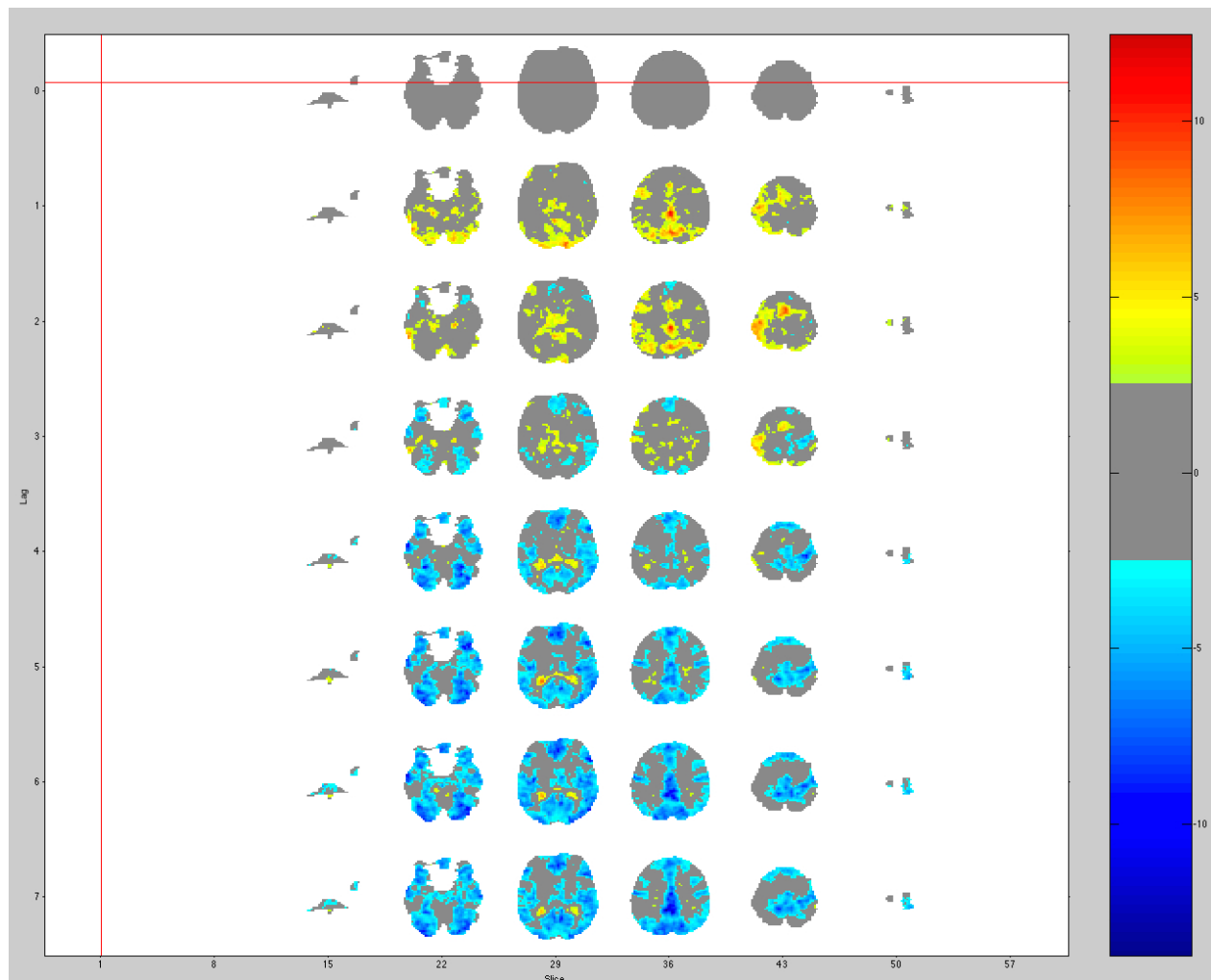
Posterior Cingulate	Left	-3	-60	6	30	-3.47	23
Caudate	Right	15	-15	18	--	-3.34	12
Supramarginal Gyrus	Left	-36	-42	36	40	-3.24	16
Putamen	Right	24	0	-6	--	-3.18	14
Medial Frontal Gyrus	Right	6	45	-9	10	-3.06	16

Note. BA = Brodmann Area, BSR = Bootstrap ratio. This cluster report was created using a minimum BSR for +/-2.5 ($p < .0124$) and a minimum cluster size 10 voxels. MNI Coordinates and BSR value are reported for cluster maxima.

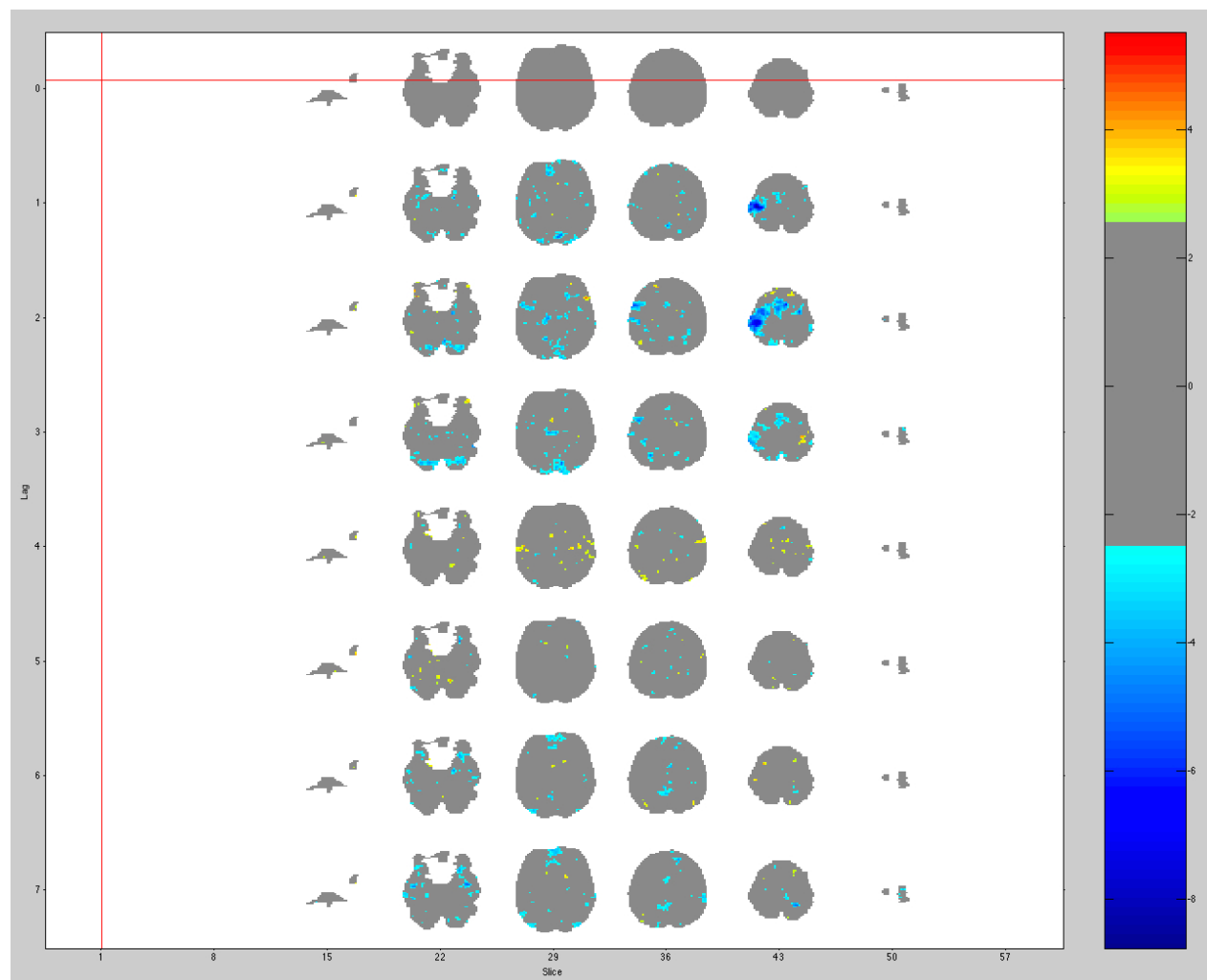
Supplementary Table 7
Full Cluster report for LV1 from the Task Switch & Control PLS Analysis

Cluster peak locations	Hemisphere	MNI Coordinates			BA	BSR	Cluster Size (in voxels)
		X	Y	Z			
Task switching							
Superior Parietal Lobule	Left	-36	-72	45	7	10.73	5957
Cingulate Gyrus	Left	0	-33	36	31	9.23	522
Cuneus	Right	9	-87	6	17	8.90	815
Thalamus	Right	9	-18	12	--	8.33	462
Inferior Temporal Gyrus	Left	-54	-48	-9	20	6.86	324
Parahippocampal Gyrus	Right	21	-24	-12	35	5.86	37
Middle Temporal Gyrus	Right	63	-45	-6	21	5.42	114
Hippocampus	Right	33	-12	-12	--	5.17	10
Putamen	Right	24	15	0	--	5.16	217
Cingulate Gyrus	Right	24	-21	33	31	4.61	20
Precentral Gyrus	Right	45	6	33	9	4.45	69
Clastrum	Left	-36	-6	0	*	4.43	31
Substantia Nigra	Left	-6	-15	-12	--	4.36	12
Superior Temporal Gyrus	Right	36	-48	18	22	4.28	21
Middle Frontal Gyrus	Right	48	36	27	46	3.65	19
Control							
Inferior Frontal Gyrus	Right	48	30	3	45	-5.68	121
Medial Frontal Gyrus	Left	-6	51	9	10	-5.05	207
Anterior Cingulate	Left	-3	33	-6	32	-4.60	19
Cingulate Gyrus	Right	15	-12	42	24	-4.60	25
Medial Frontal Gyrus	Right	6	-18	63	6	-4.18	27
Middle Temporal Gyrus	Left	-54	-12	-9	21	-4.12	19
Insula	Right	42	-15	21	13	-3.92	12
Middle Frontal Gyrus	Left	-21	30	42	8	-3.91	20
Precentral Gyrus	Right	30	-27	63	4	-3.89	25
Precentral Gyrus	Right	18	-30	69	4	-3.88	23
Inferior Frontal Gyrus	Left	-39	33	0	47	-3.80	25
Precentral Gyrus	Right	39	-18	48	4	-3.65	17
Posterior Cingulate	Right	24	-54	12	30	-3.49	10
Cuneus	Right	18	-84	30	19	-3.32	14

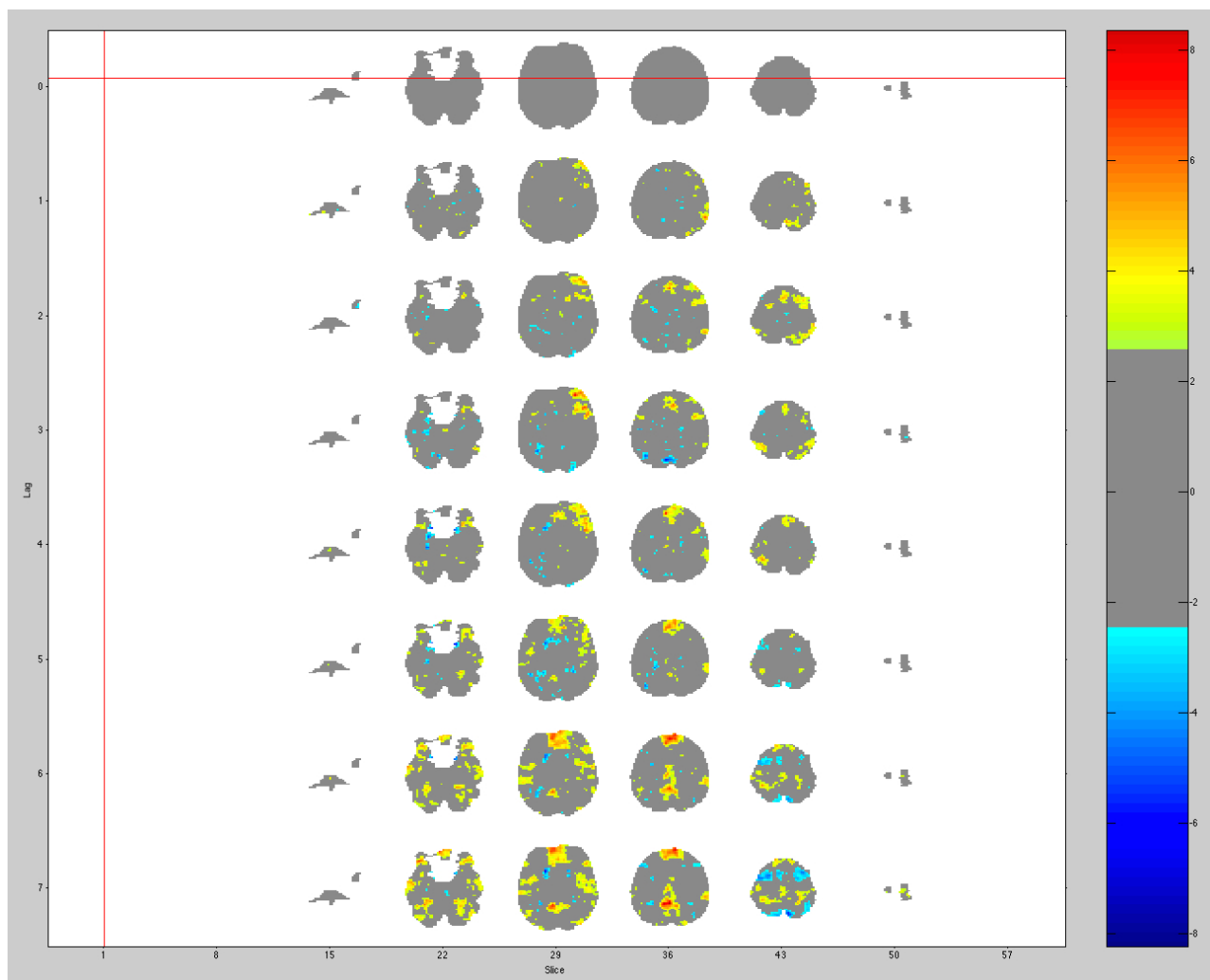
Note. BA = Brodmann Area, BSR = Bootstrap ratio. This cluster report was created using a minimum BSR for +/-2.5 ($p < .0124$) and a minimum cluster size 10 voxels. MNI Coordinates and BSR value are reported for cluster maxima.



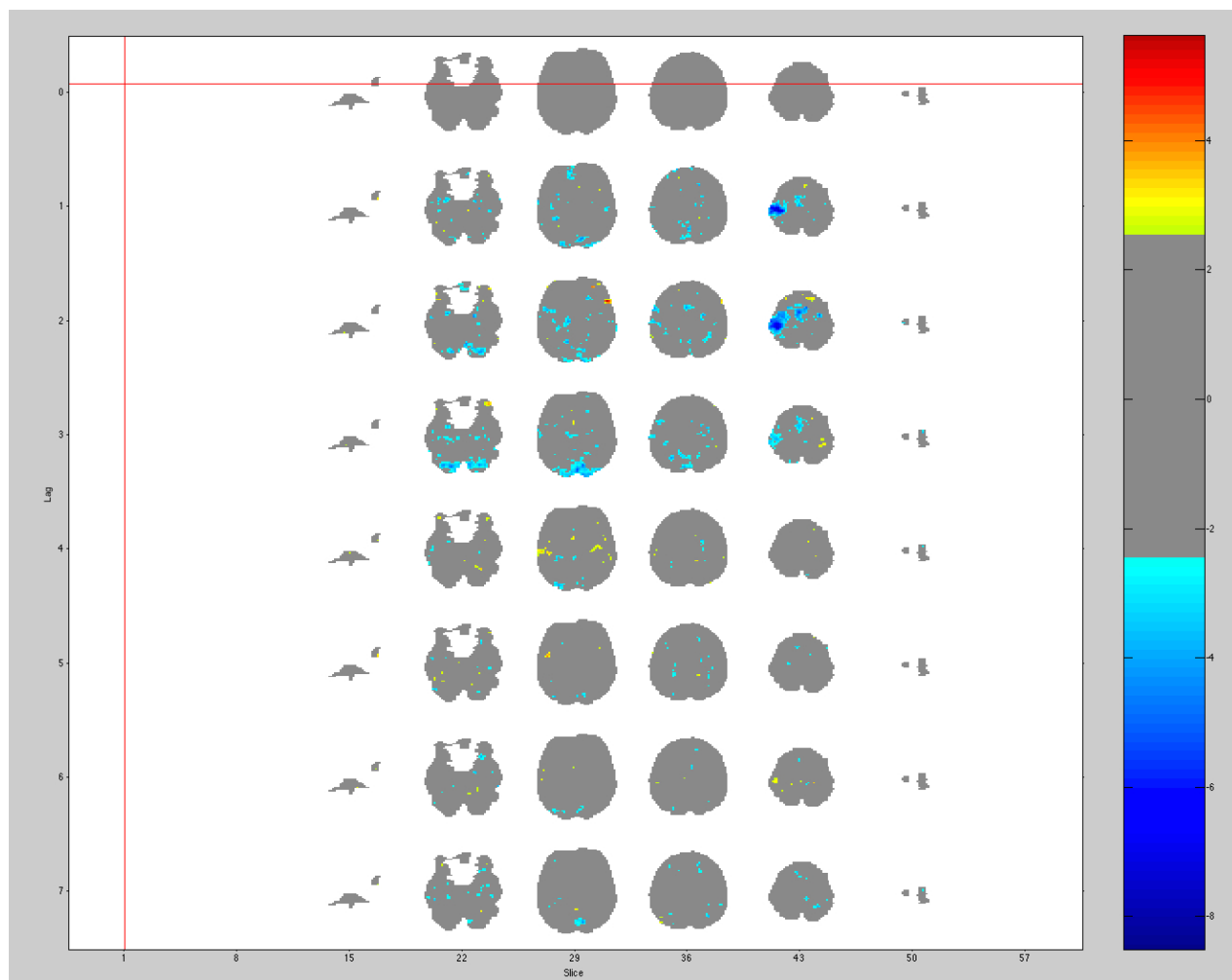
Supplementary Figure 1. Axial slices depicting the brain pattern identified by LV1 in the full-model PLS analysis, dissociating task switching (warm colours) from all other conditions (cool colours). Each row represents brain patterns associated with a different time point, from lag 0 (event onset) on the top row, to lag 7 (14s post event onset) on the bottom row. In interpreting our results, we considered findings from lag 2. Images were generated using a bootstrap ratio of ± 2.5 ($p < .0124$).



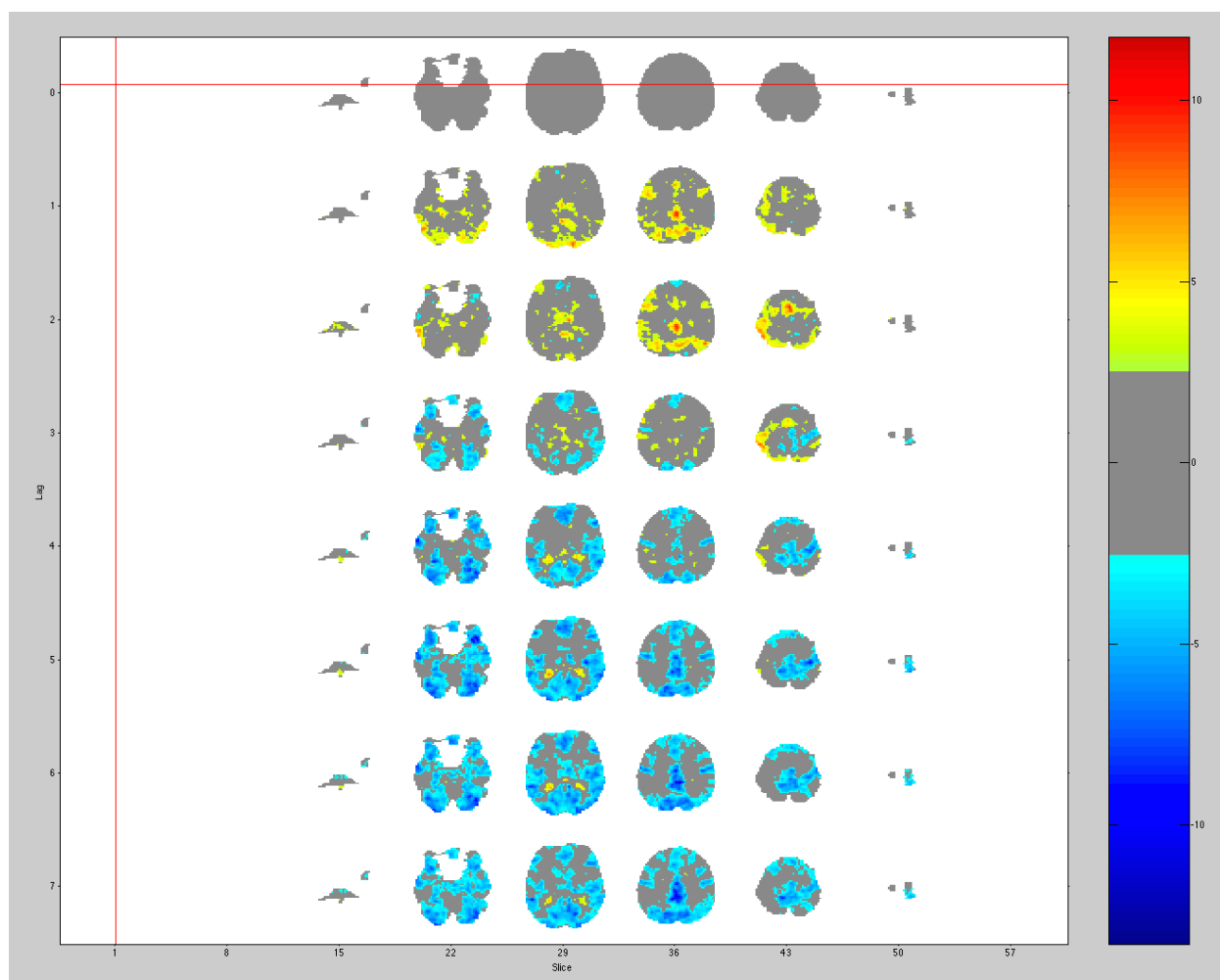
Supplementary Figure 2. Axial slices depicting the brain pattern identified by LV2 in the full-model PLS analysis, dissociating inhibition (warm colours) from all other conditions (cool colours). Each row represents brain patterns associated with a different time point, from lag 0 (event onset) on the top row, to lag 7 (14s post event onset) on the bottom row. In interpreting our results, we considered findings from lag 2. Images were generated using a bootstrap ratio of ± 2.5 ($p < .0124$).



Supplementary Figure 3. Axial slices depicting the brain pattern identified by LV1 in the PLS analysis of correct updating trials (warm colours) and control trials (cool colours). Each row represents brain patterns associated with a different time point, from lag 0 (event onset) on the top row, to lag 7 (14s post event onset) on the bottom row. In interpreting our results, we considered findings from lag 2. Images were generated using a bootstrap ratio of ± 2.5 ($p < .0124$).



Supplementary Figure 4. Axial slices depicting the brain pattern identified by LV1 in the PLS analysis of correct inhibition trials (warm colours) and control trials (cool colours). Each row represents brain patterns associated with a different time point, from lag 0 (event onset) on the top row, to lag 7 (14s post event onset) on the bottom row. In interpreting our results, we considered findings from lag 2. Images were generated using a bootstrap ratio of ± 2.5 ($p < .0124$).



Supplementary Figure 5. Axial slices depicting the brain pattern identified by LV1 in the PLS analysis of correct task switching trials (warm colours) and control trials (cool colours). Each row represents brain patterns associated with a different time point, from lag 0 (event onset) on the top row, to lag 7 (14s post event onset) on the bottom row. In interpreting our results, we considered findings from lag 2. Images were generated using a bootstrap ratio of ± 2.5 ($p < .0124$).